

AD-763 912

STABILIZATION FOR PAVEMENTS

J. L. Rice

Army Construction Engineering Research
Laboratory
Champaign, Illinois

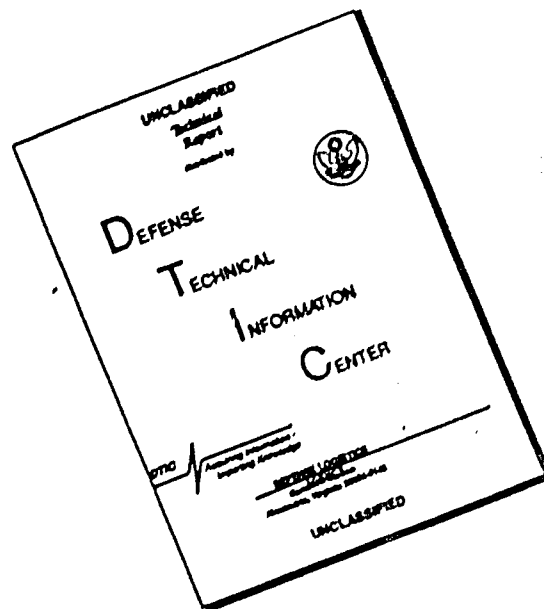
May 1973

DISTRIBUTED BY:

NTIS

National Technical Information Service
U. S. DEPARTMENT OF COMMERCE
5285 Port Royal Road, Springfield Va. 22151

DISCLAIMER NOTICE



THIS DOCUMENT IS BEST QUALITY AVAILABLE. THE COPY FURNISHED TO DTIC CONTAINED A SIGNIFICANT NUMBER OF PAGES WHICH DO NOT REPRODUCE LEGIBLY.

TECHNICAL REPORT S-11

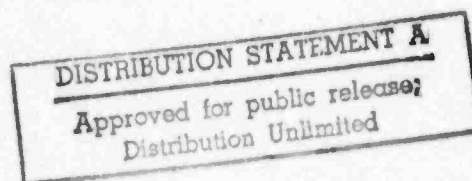
STABILIZATION FOR PAVEMENTS

by
J. L. Rice

May 1973



Department of the Army
CONSTRUCTION ENGINEERING RESEARCH LABORATORY
P.O. Box 4005
Champaign, Illinois 61820



Approved for public release; distribution unlimited.

ABSTRACT

Rigid and flexible pavement model tests were conducted to evaluate methods for assessing the structural benefits imparted to a pavement structure by stabilized elements. Current Corps of Engineers rigid pavement design and evaluation methods are based on stress in the concrete pavement as calculated by the Westergaard algorithm. This method appears applicable for pavements containing lime and bituminous stabilized layers only. Cement stabilized layers should be evaluated by an elastic layered algorithm. The California Bearing Ratio method of design and evaluation of flexible pavement structure appeared to yield satisfactory results for flexible pavements containing stabilized elements.

FOREWORD

This investigation was sponsored by the U.S. Army Corps of Engineers, Office of the Chief of Engineers (OCE), Washington, D.C. as part of Project "Investigation for Development of Engineering Criteria," under Subproject, "Soils Stabilization and Stability."

The investigation reported herein was conducted by the U.S. Army Construction Engineering Research Laboratory (CERL), Champaign, Illinois and the Ohio River Division Laboratories (ORDL), Cincinnati, Ohio during the period FY 62--FY 71.

CERL personnel actively engaged in the investigation were Messrs. J.L. Rice and J.J. Healy. Other personnel involved were: Messrs. F.M. Mellinger (ORDL Director, retired) and J.J. Scanlon (ORDL). This report was prepared by Mr. J.L. Rice.

Col. R. W. Reisacher is Director of CERL and Dr. L. R. Shaffer is Deputy Director.

CONTENTS

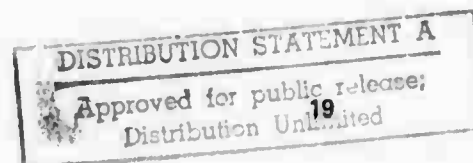
ABSTRACT
FOREWORD

iii
iv

1	INTRODUCTION	1
	Hypothesis to be Evaluated	
	Problem	
	Background	
	Scope and Objective	
	Previous Attempts to Solve	
	Theoretical Considerations	
	Prognosis	
2	APPROACH	3
	Pavement Performance	
	Types of Specimens and Tests	
	Values of Variables and Control Constants	
	Measurement Methods	
	Method of Analysis	
3	TEST PROCEDURES	4
	Specimens Prepared	
	Instrumentation Set-Up	
	Construction of the Test Models	
	Conduct of the Tests	
4	TEST RESULTS	6
5	ANALYSIS AND DISCUSSION	10
	Analysis	
	Discussion	
6	CONCLUSIONS, RECOMMENDATIONS AND CLOSURE	17
	Conclusions	
	Recommendations	
	Closure	

REFERENCES
FIGURES

DISTRIBUTION
DD FORM 1473



FIGURES

Figure		Page
1	Completed Subgrade to Placement of Polyethylene Sheeting	19
2	Coating of Crack Alarm Grid Wires with Epoxy Resin Prior to Concrete Placement	19
3	Concrete Placement Approximately One Half Complete	20
4	Vibrating Pan Type Compactor used to Compact Crushed Stone Base Course Material for Flexible Pavement Tests	20
5	Compaction of the Lime Soil Mixture with the Pneumatic Tamper	21
6	Overall View of a Completed Flexible Pavement Prior to Test Traffic	21
7	Linear Variable Differential Transformer Mounting Techniques	22
8	Typical Layout of Crack Alarm Wire Grid	22
9	Typical Oscillograph Trace from Traffic Testing of Model Pavement 12	23
10	Typical Deflection-Coverage Plot, West Slab, Nonstabilized	24
11	Typical Deflection-Coverage Plot, East Slab, Nonstabilized	24
12	Typical Strain-Coverage Plot, West Slab, Nonstabilized	25
13	Typical Strain-Coverage Plot, East Slab, Nonstabilized	25
14	Typical Deflection-Coverage Plot, West Slab, Stabilized	26
15	Typical Deflection-Coverage Plot, East Slab, Stabilized	26
16	Typical Strain-Coverage Plot, West Slab, Stabilized	27
17	Typical Strain-Coverage Plot, East Slab, Stabilized	27
18	Design Factor versus Coverages for Initial Slab Failure	28
19	Typical Summary of Load Transfer Tests Across Joint	28
20	Design Curves for Concrete Airfield Pavements, Single Wheel, 100 Sq. In. Contact Area	29
21	Nondimensional Plot of Single Wheel Design Curve and Model Test Data Using Westergaard Analysis	29
22	Close Up View of a Failed Area on Model Test 6	30
23	Close Up View of a Failed Area on a Prestressed Pavement	30
24	Summary of Rigid Pavement Tests	31
25	Consolidated CBR Curves for 5000 Coverages	31
26	Percent Design Thickness Versus Coverages—Flexible Pavement Failure	32
27	Summary of Flexible Pavement Tests	32

UNCLASSIFIED

Security Classification

DOCUMENT CONTROL DATA - R & D		
(Security classification of title, body of abstract and indexing annotation must be entered when the overall report is classified)		
1. ORIGINATING ACTIVITY (Corporate author) Construction Engineering Research Laboratory P.O. Box 4005 Champaign, Illinois 61820		2a. REPORT SECURITY CLASSIFICATION Unclassified
3. REPORT TITLE STABILIZATION FOR PAVEMENTS		2b. GROUP
4. DESCRIPTIVE NOTES (Type of report and inclusive dates) Technical Report		
5. AUTHOR(S) (First name, middle initial, last name) J. L. Rice		
6. REPORT DATE May 1973	7a. TOTAL NO. OF PAGES 32 40	7b. NO. OF REFS 14
8a. CONTRACT OR GRANT NO.	9a. ORIGINATOR'S REPORT NUMBER(S) CERL-TR-S-11	
b. PROJECT NO. Details of illustrations in this document may be better studied on microfiche.	9b. OTHER REPORT NO(S) (Any other numbers that may be assigned this report) AD# obtainable from address block 1.	
10. DISTRIBUTION STATEMENT Approved for public release; distribution unlimited.		
11. SUPPLEMENTARY NOTES Copies of this report are obtainable from National Technical Information Service, Springfield, Virginia 22151		12. SPONSORING MILITARY ACTIVITY Department of the Army
13. ABSTRACT Rigid and flexible pavement model tests were conducted to evaluate methods for assessing the structural benefits imparted to a pavement structure by stabilized elements. Current Corps of Engineers rigid pavement design and evaluation methods are based on stress in the concrete pavement as calculated by the Westergaard algorithm. This method appears applicable for pavements containing lime and bituminous stabilized layers only. Cement stabilized layers should be evaluated by an elastic layered algorithm. The California Bearing Ratio method of design and evaluation of flexible pavement structure appeared to yield satisfactory results for flexible pavements containing stabilized elements.		
14. KEY WORDS pavement model tests elastic layered algorithm flexible pavement structure		

DD FORM 1473
1 NOV 65REPLACES DD FORM 1473, 1 JAN 64, WHICH IS
OBSOLETE FOR ARMY USE.

UNCLASSIFIED

Security Classification

STABILIZATION FOR PAVEMENTS

1 INTRODUCTION

Hypothesis to Be Evaluated. The performance of pavements containing stabilized elements has been observed to be superior to the performance of similar pavements without stabilized elements.^{1,2,3} It would appear that this improved performance could be exploited in design of new pavements and in the evaluation of existing pavements. These improvements can result in large economic benefits during the life of the pavement.

Problem. The use of various stabilizers to improve soil workability and/or to enhance soil strength has been widely recognized as beneficial to pavement construction and performance. Data and analysis are lacking to determine the actual structural benefits imparted to a pavement structure by the incorporation of a stabilized element in the pavement structure. A need exists to quantify the structural benefits associated with stabilized elements and to provide a rationale which engineers can use to exploit the structural benefits derived from stabilization. Present design and evaluation procedures are limited as to the inclusion of stabilized elements in the subgrade. In the case of rigid pavement, all materials beneath the pavement slab are represented by a "k" value obtained from a plate bearing test run on the material directly below the pavement slab. For flexible pavements, the California Bearing Ratio (CBR) is used to describe the strength of pavement elements. Some stabilized layers possess sufficient rigidity and strength to exhibit some flexural action and, because the CBR test is basically a penetration test, its use in assessing the strength of a flexural type element is questionable.

Background. Various forms of stabilization have been used for some 20 to 25 years to improve soil workability and/or provide a working platform for

construction operations. At times, contractors have elected to construct a stabilized layer in order to maintain construction operations during periods of inclement weather. Stabilized layers are also constructed to provide support for construction machinery during favorable weather since construction operations result in a rather high volume of traffic during paving operations.

Generally, the performance of pavements with a stabilized element is superior to the performance of identical pavements without stabilized elements. This has been observed in surveys of actual in-service pavements.⁴ The designer is eager to exploit the improved performance associated with stabilized layers: cost reductions may be realized if a stabilized layer could be used to replace either a higher cost subbase, a select base, or to reduce the quantity of paving materials. Very little quantitative information has been available to provide the pavement designer with a rationale to assess the structural benefits associated with stabilization.

Scope and Objective. An extensive testing program has been initiated to determine the structural benefits of stabilized layers in a pavement structure and allow the designer to exploit those benefits.

Previous Attempts to Solve. Many tests have been conducted on pavements containing stabilized elements. These tests were mainly static type tests in which pavement response was measured by strain and/or deflection transducers. The results of these tests were expressed in terms of equivalency between thickness of stabilization and thickness of the base course. Base course materials are known to improve the supporting capability of subgrades; data are readily available which indicate that an increase in subgrade modulus can be expected when various thicknesses of base course materials are placed over subgrades of various strengths.⁵ By measuring the response of

¹E.L. Kawala, *Cement-Treated Subbases for Concrete Pavements*, Technical Bulletin 235 (American Road Builders Association, 1958).

²Ahlberg and Barenberg, *Pozzolanic Pavements*, Engineering Experiment Station Bulletin 473 (University of Illinois, February 1965).

³M.R. Thompson, "Lime-Treated Soils for Pavement Construction," *ASCE Proceedings, Highway Division Journal HW-2* (November 1968).

⁴E.L. Kawala, "Cement Treated Subbase Practice in U.S. and Canada," *ASCE Proceedings, Highway Division Journal HW-2* (October 1966).

⁵Soil Testing Services, Inc., *Thickness Design Procedure for Airfields Containing Stabilized Pavement Components*, prepared for the Federal Aviation Agency, Contract No. ARDS-468, AD 607331.

pavements which contain stabilized elements, a back-calculation can be performed to determine an equivalent subgrade support. Knowing the subgrade support of the indigenous materials then allows a calculation of the increase in subgrade support and a corresponding estimate of the equivalency to thickness of base course. Investigators have reported from 1:1 to 1:2 equivalency between stabilized layers and base course layers.⁶ The equivalency varies due to differing stabilizing materials, the amount of stabilizer and strength of the indigenous material.

Theoretical Considerations. Several analytical solutions are available to calculate deflections, stresses and strains in pavement structures. These solutions generally differ in the model assumed for the subgrade. The Westergaard solution assumes the subgrade behaves as a Winkler foundation while the other solutions assume an elastic subgrade representation.

Existing Corps of Engineers criteria for rigid pavements are based on the Westergaard solution with the Winkler foundation. This method also considers only a single plate of constant rigidity resting on a foundation composed of independent linear springs. No provision is made for intermediate layers, and these must be considered either in the spring constant of the foundation or in the rigidity of the overlying plate. The Westergaard solution is for a static load. Since pavements are subjected to a range of loadings, from static to dynamic, empirical adjustments have been made to establish allowable flexural stresses in rigid pavements to account for the effects of realistic loadings and environmentally imposed loadings.

Existing Corps of Engineers criteria for flexible pavements are based on the correlation between CBR and pavement performance. This correlation is largely empirical and new materials are difficult to incorporate in the present method without exhaustive performance tests. Different pavement layers can be analyzed by the CBR method by performing essentially a new flexible pavement design for each layer encountered. The method provides a total pavement thickness requirement but does not include a provision for pavement layer quality.

Some analytical techniques are available to analyze multilayered pavement structures. These analyses can

be applied to both rigid and flexible pavement structures. They require the assumption that all layers behave elastically and the loading is static. The solutions generally require the use of a digital computer as the equations are too unwieldy for hand calculation except at a very few selected points in the structure. The layered structure analyses require, as input, a value of elastic modulus and Poisson's ratio for each layer. Elastic moduli and Poisson's effects for naturally occurring and stabilized soils are extremely difficult to ascertain due to both nonlinearity and variation with time. The primary advantage in layered structure analysis is that the state of stress for the complete structure can be produced. Interface conditions as well as intermediate points can be investigated.

Two techniques are also available to determine the ultimate collapse load of rigid pavements.^{7,8} These techniques are essentially elasto-plastic analyses. The failure is assumed to be progressive and is initiated by the formation of cracks on the bottom slab surface to form plastic hinges. Further application of load causes a crack to form in the top slab surface at the point of maximum negative bending which occurs at some distance from the load. The top surface fibers are in tension rather than compression, and the progression of the negative crack is from the top surface downward. In both of these methods, the pavement is represented as a single plate resting on a dense liquid foundation. No capability of specifying more than one layer of paving material is provided. The loading is considered to be static. Normally pavements crack on the bottom slab surface, and upon further application of load the cracks migrate from the bottom to the top surface. This migration of cracking has been noted in both test track and operational pavements. The observed manner of crack propagation tends to cast doubt on the applicability of the ultimate collapse load analysis which requires the crack to propagate from the surface to the bottom of pavements subjected to rolling loads.

Prognosis. The probability of successfully quantifying the performance gains associated with a stabilized layer is good if performance data are provided for both

⁶Load Tests on Rigid Airfield Pavements Constructed on Stabilized Foundations, Unpublished Memorandum Report (Corps of Engineers, Ohio River Division Laboratories).

⁷Anders Losberg, *Structurally Reinforced Concrete Pavements*, (Chalmers University of Technology, Goteborg, 1960).

⁸J.J. Myerhoff, "Load Carrying Capacity for Concrete Pavements," *ASCE Proceedings*, Vol 88, No. SM-3 Part I (June 1962).

pavements with and without stabilized elements. A direct comparison should provide a basis for determining the performance benefit and the opportunity to assess the in-use empiricism for pavement design and evaluation.

2 APPROACH

Pavement Performance. Pavement performance is the prime attribute to be measured in this study. Unfortunately, performance can be a rather nebulous and elusive characteristic. The current Corps of Engineers pavement design and evaluation methods incorporate pavement performance by establishing a structural failure criteria and then by determining the magnitude and number of repetitions of load required to produce the various degrees of failure as defined in the criteria. Failure of any pavement is a progressive phenomenon as opposed to a catastrophic event such as might occur when a structural member in a building fails. Very few catastrophic pavement failures have been reported. And, since failures of this type are extremely rare, they are not included in the normal failure criteria. Three conditions of failure have been established for rigid pavements as follows:

Initial Failure Condition. The initial failure condition is defined as that point in the life of the pavement when 50 percent of the slabs in the traffic area are divided into two to three pieces by cracks that extend entirely through the slab and which were the result of traffic loading rather than shrinkage, or other nontraffic-induced stresses. This condition was defined to mark the beginning of structural failure and to signal that the pavement should be closely watched as the progression of deterioration will be rather rapid from this point.

Shattered Slab Condition. The shattered slab failure condition is defined as that point in the life of a pavement when the slabs in the traffic area are divided into six pieces by cracks extending entirely through the thickness of the slab and were the result of traffic loading. This condition was defined to mark the point at which an overlay or some major strengthening program should be undertaken if the pavement is expected to continue to provide service.

Complete Failure Condition. The complete failure condition is defined as the point at which the

pavement is no longer serviceable and is said to occur when the slabs in the traffic area are broken into approximately 35 pieces (each piece being about 15-20 square feet in area). This condition was defined to mark the end of a pavement's useful life. Operations from a pavement in this condition are no longer feasible due to safety and comfort considerations.

Flexible pavement failure is considered to occur at that level of traffic which produces either of two failure conditions: when surface upheaval of the pavement adjacent to the traffic lane reaches one inch or more, or when surface cracking progresses to the point that the pavement is no longer waterproof.

Pavement performance is judged by the magnitude of load and number of repetitions required to produce one of the conditions of failure described above. Repetitions of load are expressed in terms of coverages. A coverage is said to have occurred when each point in the traffic area has been subjected to maximum stress by a single pass of the load wheel. The coverage concept of describing traffic volume is used because of the random nature of aircraft traffic. Traffic is normally distributed across a finite width of pavement and the coverage method of describing traffic provides a common base for representing traffic intensity.

Types of Specimens and Tests. Because of the high cost associated with constructing and testing full scale pavements and because of the weather dependency for this type of testing, small scale model testing was selected as the most economical method of test. A small scale test apparatus was available from a previous study of prestressed pavements.⁹ The apparatus consisted of a soil bin 8 feet wide, 16 feet long and 4 feet deep which rested on a concrete floor. A loading device was designed to operate in the longitudinal direction on railroad rails located on top of the soil bin walls. The loading device was powered by a 3-horsepower electric motor. The loading box was moved laterally across the pavements by a ½-horsepower electric motor. The load was applied to the pavement by a single wheel. For rigid pavement tests, a cushion tire was used for trafficking. A pneumatic tire was used for flexible pavement testing. The cushion tire is capable of loadings up to 3000 pounds and the pneumatic tire

⁹Small Scale Model Studies of Prestressed Rigid Pavements-Part I, Development of the Model and Results of Exploratory Tests, Technical Report No. 4-13/AD281580 (Ohio River Division Laboratories, May 1962).

is capable of loadings up to 1800 pounds. The cushion tire was not suitable for use on flexible pavements due to the high contact pressures developed. The flexible pavement surface was not stable enough to withstand the range of contact pressures encountered (90-300 psi).

Test pavements were constructed so as to provide a direct comparison between pavement performance for a pavement with and without a stabilized element. One half of the pavement contained a stabilized layer and the second half did not. The pavements were trafficked in such manner that direct performance comparisons were possible by trafficking both the stabilized and unstabilized pavements in each pass.

Values of Variables and Control Constants. A large number of variables were considered to affect the results of these tests. To provide a cohesive test series and to facilitate analysis of results, several of these variables were held constant in so far as possible: concrete flexural strength, crushed stone quality and gradation, compactive effort applied and moisture content of the crushed stone, subgrade moisture content, subgrade strength for clay and granular materials, and loading rig speed. The test variables included stabilized layer thickness, total pavement structure thickness, and in some cases percentage of stabilizer material used.

Measurement Methods. The test pavements were trafficked to failure and the behavior observed. The traffic passes were counted by an electrical counter. This method was used for the rigid and flexible pavements.

Rigid pavements were instrumented with electronic transducers to measure deflection of both the elastic and residual type. Electrical strain gages were also used to determine strains in the concrete slabs. Strain gages were mounted on the top slab surface of all slabs and on the bottom slab surface of two test slabs, 11 and 12. A technique was devised during the program to determine bottom surface cracking in rigid pavements. The principle behind the technique was the interruption of electrical current by cracks forming in the concrete slab. Complementary strain data were also collected from mechanical extensometers during static loading tests to ultimate collapse. Subgrade strength was measured in terms of the modulus of subgrade reaction, k , for the rigid pavements.

Flexible pavements posed a difficult problem for instrumentation. The flexible pavement materials do not offer the chance to obtain a rigid mounting for the

linear variable differential transformer (LVDT) transducer. Proper operation of the LVDT transducer requires firm anchorage in the horizontal plane which was not available in the flexible pavement structures. Without firm anchorage, some component of horizontal movement may be reflected in the LVDT output. In one instance, a transducer was installed in the flexible pavement structure. In all cases residual deflection was obtained using conventional surveying techniques. Mechanical extensometers were also used to measure deflections during ultimate collapse load tests. Subgrade, stabilized layer and base course strength were measured by the CBR test method.

Method of Analysis. Test results were analyzed by current Corps of Engineers pavement design and evaluation methods. This provided an indication of the applicability of current methods to pavements containing stabilized elements. Another analysis technique being used is the layered elastic. Unfortunately, because of the cost of each individual test item, very little replicate data are available for a statistical analysis. Non-dimensional expressions for data will, however, assist in developing a base for interpolation and extrapolation of data. A brief presentation of dimensional analysis and similitude as applied to this problem will assist in the application of these tests to actual pavement structures.

3 TEST PROCEDURES

Specimens Prepared. A total of 34 pavement tests were conducted. Of this group, 20 were rigid pavements and 14 were flexible pavements. The rigid pavement test program included both clay and granular subgrades. Tests conducted on the clay subgrade were: 7 lime stabilization tests, 9 cement stabilization tests, 2 bituminous stabilization tests. Two tests were conducted on the granular subgrade using cement stabilization. The flexible pavement testing program was conducted with a clay subgrade and granular subgrade. Tests conducted with the clay subgrade were: 6 lime stabilization tests, 4 cement stabilization tests, 2 bituminous stabilization tests. Two tests were conducted over the granular subgrade using cement stabilization.

The construction of a typical test rigid pavement is shown by the sequence of photographs in Figures 1, 2

and 3. The construction of a typical flexible test pavement is shown in Figures 4, 5 and 6.

Construction control specimens of concrete and stabilized soil were prepared as the test pavements were constructed to provide preliminary information to be used in establishing trafficking loads. A minimum of 9 concrete control beams and 12 unconfined compression test specimens of stabilized soil were prepared for each concrete test pavement. Twelve unconfined compression test specimens of stabilized soil were prepared for each flexible test pavement.

Instrumentation Set-Up. The instrumentation set up used for the rigid pavement test series is described for each transducer used.

Deflection Transducers (LVDT Gages). Two different mounting schemes were used for these transducers. Initially the transformer was housed in a brass fixture which was cast in the concrete slab and acted as an integral part of the slab. A ferrous core was mounted on top of a brass reference rod which extended through the subgrade and rested on the concrete floor beneath the soil bin enclosure. The second mounting scheme positioned the transformer on top of the brass reference rod and the ferrous core was rigidly housed in the concrete slab. A drawing of the two different mounting methods is shown on Figure 7. The transformer signal was carried from the transducer by shielded cable to the west edge of the testing device. The shielded cable was then threaded through electrical conduit to the instrumentation room which housed the oscillograph and signal conditioning equipment. For rigid pavements subjected to interior loading one LVDT gage was installed in the center of the traffic area on the stabilized and unstabilized portions of the pavement respectively. Jointed edge pavements were instrumented with one LVDT gage on either side of the joint on both the stabilized and unstabilized portions for a total of four gages. Free edge loaded pavements contained a total of four gages, one in the center of the traffic area and one a nominal 1½ inches from the free edge, on both the stabilized and unstabilized portions. A maximum of four LVDT gages could be recorded on the oscillograph simultaneously.

Strain Gages. All strain gages were of the resistive wire type construction. The active length of the strain gages was 1 inch. The maximum aggregate size used in the portland cement concrete slabs was ½ inch. The 1-inch gage length was chosen to provide a minimum 2:1 ratio of gage length to aggregate size. Strain gages

were attached to the top slab surface as close as possible, about 1/8 inch, to the traffic area. No strain gages were used during the interior loading studies due to lack of proper recording equipment. The jointed edge pavements were instrumented with a total of four strain gages, one on either side of the joint and on both the stabilized and unstabilized portions. The free edge pavements generally were instrumented with six strain gages. One gage was located just outside the traffic area toward the slab interior, one gage was located just outside the traffic area toward the free edge if space permitted and a strain gage was attached to the vertical free edge as near as possible to the extreme fibers on the tensile side of the natural axis. This scheme was followed for both the stabilized and unstabilized portions of the pavement. Strain gage signals were carried by shielded cables and through electrical conduit to the instrumentation room. Continuous recording was obtained with the oscillograph and when more strain gages were used than could be recorded on the oscillograph, a precision switch was available to select gages at will.

Crack Alarm System. The crack alarm system was perfected about half way through the test program. The function of this device was to detect cracks in the bottom surface on the concrete test slabs. The device was intended to provide data on the length of time required for a crack in the bottom of the slab to migrate from bottom to top. Cracks in the top slab surface were detected visually. The alarm system consisted of a grid of flat copper wires cast into the bottom slab surface. The flat wires were produced in-house by cold rolling 20-gage (32 mils) enameled copper wires to a thickness of 3 to 4 mils. The cold rolling produced a brittle wire with practically no plastic range. Commercially available flat copper wire was tested in the laboratory and exhibited nearly 800 percent elongation at rupture. The cold rolled material exhibited about 20 percent elongation at rupture. Both materials failed at about 4 pounds total tensile load. Prior to casting the rigid pavements on the prepared subgrades, a 4 mil polypropylene sheet was placed over the subgrade to reduce moisture loss. The crack alarm wire grid was formed on top of the polypropylene sheet.

Two grid layout schemes were tried. The first was a rectangular grid with the wires placed in the longitudinal and transverse directions of the slab. The second was again a rectangular grid but with the wires placed diagonally across the slab at a 45° angle. The

grid was spaced at one foot intervals as shown in Figure 8. The diagonal grid was considered superior because transverse and longitudinal cracks could be detected earlier and with greater certainty than with the longitudinal and transverse grid. The wire grid was coated with epoxy resin just prior to concrete placement. The use of epoxy resin was considered necessary to achieve good bond with the concrete slabs.

Construction of the Test Models. Each test was designed to encompass the desired parameters and not to exceed the capacity of the test facility. Stabilized layer thicknesses and surface pavement thicknesses were selected to represent realistic ratios of surface/stabilized layer typical of field placement. The strength of the overall pavement was estimated and planned not to exceed the 3000-lb capacity of the facility for rigid pavements and the 1800-lb capacity for flexible pavements.

The stabilized layer placement techniques varied somewhat depending on the material. Prior to testing with lime stabilized layers, laboratory tests were performed to determine the optimum lime content for the clay material. These tests indicated that 6 percent lime by dry weight was the optimum lime content for this material. All lime stabilized layers were prepared using 3 percent lime for fixation and 3 percent lime for strength gain. Lime stabilized layers were prepared over a 3-day period. Lime in sufficient quantity to achieve fixation was thoroughly mixed with the clay and the material was then covered and allowed to cure for two days. On the third day lime was again added in sufficient quantity for strength gain and was immediately compacted in place with pneumatic tampers. Cement stabilized layers were prepared by mixing in a conventional concrete mixer and placing on the prepared subgrade in wooden forms. Consolidation of the cement stabilized layer was accomplished with surface vibration. Bituminous stabilized layers were mixed in a conventional drum type concrete mixer with the aggregate and bituminous material both heated to about 250°F. After mixing, the material was placed immediately and consolidated with a pan type vibrator.

The pavement surfacing material for the rigid pavements was a conventional type of concrete with small aggregate and high early strength Type III cement. The placement of the material was accomplished using surface trowel finish. Moist curing was used for the first 7 days and the slabs were air cured until traffic tested. In the case of jointed edge model pavements, the joint was always a longitudinal joint

with dowels used for the load transfer mechanism. Doweled joint design for the model pavement was based on shearing forces acting along the joint. The same cross-sectional area of steel dowels per unit length of slab was provided in the model pavement as would be required in a prototype slab. Dowel diameter was controlled by the maximum size of coarse aggregate used. Sufficient space was provided between the top and bottom slab surface for the dowel to accommodate the maximum particle size of coarse aggregate as well as to allow additional space equal to one half that same particle size for cement paste. These dimensions discouraged segregation of the concrete in the vicinity of the dowels. The flexible pavements were constructed of high quality crushed limestone and placed at a moisture content of about 6 to 7 percent. The material was compacted with a pan type vibrator. The pavement structure was allowed to air dry for at least three days before traffic testing was initiated.

Conduct of the Tests. Traffic was initiated with a single wheel load, which was determined by using the strength of the construction control specimens and estimating the load failure relationships at several thousand passes. An attempt was made each time a load was determined for trafficking to select a load which would fail both the stabilized and nonstabilized portions of the pavement within a reasonable time period. Often it became necessary to increase the load during the test when, after several thousand passes, it became obvious that failure could not be achieved within a reasonable length of time. All instrumentation was monitored during the trafficking portion by oscillograph recording.

4 TEST RESULTS

A narrative description of the performance of each of the 34 tests will not be presented; instead, summaries of all test results appear in Tables 1 and 2.

Table 1 contains the summary information for all rigid pavement tests. Column captions are briefly described to define and clarify the terminology.

Test Number and Section. Tests are sequentially numbered for referencing convenience; the section refers to the stabilized or nonstabilized half of the test pavement.

Table 1
Summary of Model Tests Results for Rigid Pavements

Test No. & Section	Subgrade Soil	Loading Condition	Stabilizing Agent	Thickness In.		Subgrade Modulus psi/in.		Flexural Strength psi	Bottom Slab Cracking lbs. Load	Initial Failure lbs. Load		Complete Failure lbs. Load		Remarks
				Pavement	Base	Subgrade	Base			Coverages	Coverages	Coverages	Coverages	
1. Stabilized Nonstabilized	Clay	Interior	Cement	1.04	1.08	75	N/A	890	t	1518	163	1518	350	
				2.09	None	80	N/A	763	t	2576	5119	2974	5345	
2. Stabilized Nonstabilized	Clay	Interior	Cement	1.11	1.15	80	N/A	674	t	2057	435	2037	735	
				1.45	None	80	N/A	633	t	2037	72	2037	220	
3. Stabilized Nonstabilized	Clay	Interior	Cement	1.06	2.11	80	N/A	840	t	1899	5710	1899	6000	
				1.41	None	80	N/A	676	t	1899	100	1899	280	
4. Stabilized Nonstabilized	Clay	Interior	Cement	1.07	2.21	82	N/A	940	t	1800	542	1800	1743	
				1.77	None	82	N/A	763	t	2225	5252	2225	8857	
5. Stabilized Nonstabilized	Clay	Interior	Lime	1.10	2.00	85	240	752	t	2015	2219	2015	2734	
				1.10	None	85	N/A	752	t	1005	528	1005	7040	
6. Stabilized Nonstabilized	Clay	Interior	Lime	1.00	1.00	113	200	859	t	1155	664	1400	3622	
				1.90	None	115	N/A	809	t	1155	4630	1400	979	
7. Stabilized Nonstabilized	Clay	Interior	Lime	1.10	5.00	105	135	817	t	1275	2240	1275	8004	
				1.12	None	103	N/A	857	t	1273	239	1275	1896	
8. Stabilized Nonstabilized	Clay	Jointed Edge	Lime	1.75	2.00	51	80	785	t	2203	736	2205	1503	
				1.75	None	36	N/A	647	t	2203	593	2203	553	
9. Stabilized Nonstabilized	Clay	Free Edge	Lime	1.75	3.00	47	88	798	1200 2100	2600	1900	2600	2100	
				1.75	None	58	N/A	812	1700 2000	2700	1245	2200	1200	
10. Stabilized Nonstabilized	Clay	Free Edge	Lime	1.00	1.00	118	114	914	Not Used	1621	5646	1621	7752	
				1.00	None	77	N/A	921		1007	330	1007	400	
11. Stabilized Stabilized	Clay	Free Edge	Lime	1.00	1.00	72	210	976	1763 3350	1492	1465*	1761	8700	*Drainage Crack
			Cement	1.00	1.00	72	N/A	941	1492 256	1492	400	Did Not Fail		
12. Stabilized Nonstabilized	Clay	Free Edge	Cement	1.0	1.0	67	N/A	1101	Not Used	1000	400	1500	695	
				1.50	None	67	N/A	1095		2400	2715	2400	2752	
13. Stabilized Nonstabilized	Clay	Free Edge	Cement	1.0	1.0	87	N/A	740	1504 1	1504	1	1902	1910	
				1.125	None	100	N/A	773	1231 2200	1731	5240	1902	6610	
14. Stabilized Nonstabilized	Clay	Jointed Edge	Cement	2.5	1.5	101	N/A	926	Not Used	Did Not Fail		3066	3000*	*Traffic Induced No Failure
			Modified	2.5		120	N/A	916		2755	6690	3066	17500*	
15. Stabilized Nonstabilized	Clay	Jointed Edge	Cement	1.56	0.75	253	N/A	799	1432 1729	2368	100	2368	150	
			Modified	1.53		200		745	1103 3259	2368	130	2368	130	
16. Stabilized Nonstabilized	Clay	Jointed Edge	Bituminous	1.00	1.0	91	10"	620	1805 10	1805	51	1805	78	
				1.00	1.0	97	120	584	1805 11	1805	51	1805	81	
17. Stabilized Nonstabilized	Clay	Jointed Edge	Bituminous	1.11	1.0	94	98	846	1503 115	1503	5091	1503	3388	
				1.25	1.0	102	114	862	1303 92	1303	3689	1503	5617	
18. Stabilized Nonstabilized	Clay	Jointed Edge	Bituminous	1.50	0.75	75	88	672	1905 187	2520	12	2520	103	
				1.50	0.75	120	96	627	1503 775	2520	1	2520	30	
19. Stabilized Nonstabilized	Sand	Jointed Edge	Cement	1.00	0.5	247	-	805	1945 681	1445	2155	1445	6428	
				1.00	-	333	-	755	1445 675	1445	1620	1445	1800	
20. Stabilized Nonstabilized	Sand	Jointed Edge	Cement	3.09	1.00	265	-	374	1500 545	1300	1382	2000	550	
				1.15		340	-	655	1114 416	1114	1090	1114	1500	

* Keyed to information in Failure Load and/or Failure Coverages columns.
† Crack slabs had not been developed at this stage of the study.

Reproduced from
best available copy.

Subgrade Soil. Two different subgrade materials were studied, a low strength clay and a medium strength granular material.

Loading Condition. Three different classes of loading were applied to the rigid pavement test sections: interior loading, where loads were applied at a considerable distance from an edge; jointed edge, where loads were applied in the vicinity of a doweled longitudinal construction joint; and free edge, where loads were applied to within approximately one inch of a free longitudinal edge.

Type of Stabilization. Lime, cement, and bituminous stabilizers were used to produce the stabilized element.

Thickness (pavement and base). The thickness of the rigid pavement slab and the stabilized element is given in inches.

Subgrade Modulus (subgrade and base). The modulus of the subgrade material, and the modulus measured at the top of the stabilized element are given where applicable. These values were determined from conventional plate bearing tests conducted with the 30-inch diameter plate and are in pci. The use of a 30-inch diameter bearing plate in a 48-inch deep soil bin was investigated by Ahlberg and Barenberg.¹⁰ Ahlberg and Barenberg concluded that the pressure bulb as defined by Terzaghi does not touch the bottom of a 48-inch deep soil bin and the boundary effects are therefore negligible.

Flexural Strength. After traffic testing the pavements, beams were sawed from the unfailed portions of the slabs and failed in flexure; the flexural strengths are obtained in psi.

Bottom Slab Cracking. The load and number of coverages necessary to cause an indication of slab cracking with the crack alarm device are shown. The load is the number of pounds on a single wheel, and coverages are dimensionless. The number of coverages is actually an equivalent number of coverages. If the pavement had been subjected to some loading less than the load shown, the prior loadings are accounted for in the number of equivalent coverages by using Miner's hypothesis, which assumes damage is cumulative and linear.

Initial Failure. Identical to Bottom Slab Cracking, except the crack must be visible on the top slab surface. As before, equivalent coverage levels are shown.

Complete Failure. Identical to Bottom Slab Cracking, except the failure condition is changed and the degree of distress is much higher.

In addition to the collection of data presented in Table 1, behavioral data were collected from the instrumentation transducers. Strain and deflection were measured on most of the rigid pavement model tests. These data were collected on a recording oscillograph and manually reduced at selected intervals. A copy of a typical recording trace is shown as Figure 9. The trace labeled "vertical movement of load rig" is misleading, in that the model pavement profile was not as rough as this trace would indicate. The loading frame was contained rather loosely in the unit which provided longitudinal and transverse movement. The trace shown is mainly indicating the rocking back and forth of the loading frame in the power unit, which was due to the mechanical connections between the two. The other traces show deflection or strain as appropriate, and the peak values were obtained when the load wheel was in close proximity to a transducer. Two nearly equal maximum excursions are indicative of a pass of the load wheel heading north then reversing and heading south. During this time the load was also moving laterally a small amount and the two peak readings are nearly equal. Other lesser excursions were recorded when the load wheel moved laterally, east or west, away from the transducer. The bottom line which shows as a straight narrow line with periodic wide short pulses is a timing line. The time interval between pulses is 1 minute. These data were collected, reduced and plotted. A series of typical results are shown as Figures 10 through 17. These results are for maximum values only.

Table 2 contains summary information for all the flexible pavement tests; column captions are briefly described.

Test Number and Section. The tests were sequentially numbered for referencing, and the sections were identified as either stabilized or nonstabilized.

Subgrade Soil. The majority of the tests were conducted on a low strength clay subgrade; two tests were conducted on a medium strength granular subgrade.

¹⁰ Ahlberg and Barenberg, *The U of I Pavement Test Track—A Tool for Evaluating Highway Pavements* (University of Illinois Engineering Experiment Station, January 1963).

Test No. & Section	Subgrade Soil	Load Wheel	Stabilizing Agent	Thickness in.		CBR Percent		lbs. Load	Failure Coverages		Remarks
				Cr. Stone	Stab.	Subgrade	Stab. Cr. Stone				
1. Stabilized Nonstabilized	Clay	Cushion Tire	Lime	3 5	2 -	4 4	9 21	1008* 1008*	25* 25*		*Failure in Cr. Stone
2. Stabilized Nonstabilized	Clay	Cushion Tire	Lime	3 5	2 -	4 4	10 44	1008* 1008*	1050* 1050*		*Failure in Cr. Stone
3. Stabilized Nonstabilized	Clay	Cushion Tire	Lime	2 4	2 -	5 5	12 100	2997* 1997*	141* 54*		*Failure in Cr. Stone
4. Stabilized Nonstabilized	Clay	Pneumatic 60 psi	Lime	2 3	1 -	6 6	20 34	1492 1492	803 803		*Did not Fail - exceeded capacity of load rig
5. Stabilized Nonstabilized	Clay	Pneumatic 70 psi	Lime	2-1/2 3	1/2 -	6 6	12 21	1508 1508	2595 660		
6. Stabilized Nonstabilized	Clay	Pneumatic 70 psi	Lime	1-5/8 2-1/4	7/8 -	5 5	9 8	1559 1559	285 62		
7. Stabilized Nonstabilized	Clay	Pneumatic 70 psi	Cement	1-1/2 3	1/2 -	10 7	2 15	1699 1699	246 214		*Did Not Fail
8. Stabilized Nonstabilized	Clay	Pneumatic 65 psi	Cement	2-1/2 3	1/2 -	4 3	5 12	743 743	186 149		
9. Stabilized Nonstabilized	Clay	Pneumatic 65 psi	Cement Modified	2 3	1 -	7 5	17 33	1090 1090	399 78		
10. Stabilized Nonstabilized	Clay	Pneumatic 65 psi	Cement Modified	2-1/2 3	1/2 -	7 7	13 32	1197 1854	246 214		
11. Stabilized Nonstabilized	Clay	Pneumatic 65 psi	Bitum	2-1/4 3-1/4	1 -	4 2	22 25	1015 1015	88 61		
12. Stabilized Nonstabilized	Clay	Pneumatic 70 psi	Bitum	2-3/8 4	1-5/8 -	3 2	4 26	1100 1100	471 287		
13. Stabilized Nonstabilized	Granular	Pneumatic 70 psi	Cement	1-1/2 2-1/4	3/4 -	7 19	58 30	1753 1325	2278* 8		*Traffic directly on Stab Material
14. Stabilized Nonstabilized	Granular	Pneumatic	Cement	1-1/2 2	1/2 -	8 8	47 22	2236 1300	332 134		

NOTE: Asterisks keyed to information in Failure Load and/or Failure Coverages columns.

Table 2
Summary of Model Tests Results for Flexible Pavements

Load Wheel. Early tests were attempted with the cushion tire which was used for rigid pavement tests. Later the loading rig was modified to accept a pneumatic tire which was operated between 60 and 70 psi inflation pressure.

Type of Stabilization. Stabilizer used to produce the stabilized element under investigation.

Thickness (crushed stone, stabilized element). Presents, in inches, the thicknesses of crushed stone over the natural subgrade and over the stabilized element, and also the thickness of the stabilized element. It should be noted that the total pavement thickness over the subgrade was held constant on both the stabilized and nonstabilized portions of the pavement. The stabilized element thus replaced an identical thickness of high quality crushed limestone.

Subgrade CBR (stabilized, crushed stone). Values of measured CBR are tabulated for the natural subgrade, for the stabilized element over the natural subgrade, and for the surface of the crushed stone, over the natural subgrade and over the stabilized element.

Failure (load and coverages). These values show the load and coverages necessary to produce failure as defined previously. As with the rigid pavement tests, the coverages have been adjusted using Miner's hypothesis to account for loadings other than the failure load.

5 ANALYSIS AND DISCUSSION

Analysis.

Rigid Pavement Tests. The current Corps of Engineers rigid pavement design and evaluation criteria are based on the Westergaard analysis for pavement stresses.¹¹ Through full scale traffic tests of rigid pavements, empirical relationships have been established which allow a static analysis to be used for dynamic, fatigue and environmentally imposed loadings. Stress in a rigid pavement structure is calculated by the Westergaard static loading method and compared to the modulus of rupture of the concrete paving material. A design factor or, more commonly, a safety

factor is then established by dividing the modulus of rupture by the calculated flexural stress, and pavement life predictions are made based on the magnitude of the design factor. Figure 18, which reflects the total C of E test track experience, shows the relationship between design factor and coverages for the initial failure condition. For "k" values in the 300 to 500 pci range, a thickness reduction, and conversely a reduction in design factor, is allowed based on observations of full scale pavements which indicate that while slab cracking will occur, the rate of deterioration is slow due to superior subgrade support.

The model pavements trafficked under interior loading conditions were analyzed as follows.

The maximum flexural stress under load is calculated by the Westergaard interior load formula:

$$\sigma = \frac{P}{h^2} \left[0.275 (1+\mu) \log \frac{Eh^3}{k(\frac{a+b}{2})^4} \pm 0.239 (1-\mu) \frac{(a-b)}{(a+b)} \right] \quad [\text{Eq 1}]$$

where σ = flexural stress in the extreme slab fibers,
psi

P = wheel load, lbs

h = slab thickness, inches

E = modulus of elasticity for slab material,
psi

μ = Poissons ratio for the slab material,
no units

k = modulus of subgrade reaction, pci

a,b = major and minor axes of assumed
elliptical contact area, inches

The loads used for the calculation of flexural stress were the loads which caused initial failure of the slabs. Table 3 lists the results of these calculations for the pavements without a stabilized element.

These analyses compare the performance of the model test pavements with the performance which would be predicted by the current Corps criteria. Referring to Figure 18, it becomes apparent that the model pavements should have all failed at less than 10 coverages. The observed performance indicates the design factors are smaller than expected and the induced stresses are approximately one-half what would be expected. The absence of environmental effects undoubtedly caused the model pavements to perform better than anticipated; however, the superior performance observed was considered much better than that expected because of the absence of environmental effects.

¹¹ H.M. Westergaard, *Stresses in Concrete Pavements Computed by Theoretical Analysis*, Highway Research Board Paper (December 1925).

Table 3

Test Number	Wheel Load	Slab Thickness	Subgrade Modulus	Flexural Stress	Modulus of Rupture	Design Factor
1	2974	2.09	80	1050	765	.73
2	2037	1.45	80	1388	653	.47
3	1899	1.41	80	1365	676	.50
4	2223	1.77	82	1068	765	.72
5	1005	1.10	85	1157	752	.65
6	1155	1.00	115	1493	880	.59
7	1275	1.12	103	1368	857	.63

Rigid pavement model tests were also conducted on free edge and jointed edge pavements. The analysis of these tests was identical to that of the interior loaded pavements except that Westergaard's edge loading equations were used in place of the interior loading equations. For free edge pavements, the analysis was straight forward, but the analysis of the jointed edge pavements required the use of a load transfer factor. The load transfer factor is an indicator of the amount of load which is transferred from the loaded slab to the unloaded slab by the jointing mechanism. Several load transfer measurements were made on jointed rigid pavements. As would be expected, load transfer tended to decrease with increased traffic and deterioration. A typical result of such load transfer tests is shown on Figure 19. These tests were conducted by placing the load tangent to the jointed edge and measuring strain in the loaded and unloaded slabs. The strain readings were used to determine the percentage of the load carried by the loaded and the unloaded slabs respectively. In the analyses of jointed edge pavements, the joints were assumed to transfer a constant 25 percent for stabilized sections and 20 percent for nonstabilized sections. These values are considered typical for the entire life of the pavement. Current Corps criteria assumes an average load transfer value of 25 percent for operational pavements. The analysis of free edge and jointed edge pavements using the Westergaard analysis yielded results similar to those found for the interior loading conditions. The calculated stresses were about twice the observed values, based on pavement performance.

The Corps of Engineers criteria utilize tensile stress generated in the slab in the flexural response mode as a basis of performance analysis. Tensile stress, which is maximized at the edge load position, is assumed to be the controlling stress in rigid pavement performance.

This tensile stress is compared with the modulus of rupture of the concrete paving material to define the relationship between allowable loads and repetitions of load. The modulus of rupture is determined by the conventional third point loading of a beam. This information provides a basis for establishing a relationship between flexural stress expressed as a ratio of the modulus of rupture and repetitions of load.

Assuming the tensile stress due to flexure is the controlling stress in a rigid pavement, a dimensional analysis based on flexural stress is required to model pavement behavior. Langhaar¹² has proposed a dimensional analysis of stresses in an airport pavement. Langhaar assumes that stress in a pavement slab is a function of: applied load, F , slab thickness, h , contact pressure, p , subgrade modulus, k , and the modulus of elasticity of the concrete slab, E . Langhaar proposed an equation of the form:

$$\sigma = \frac{F}{h^2} f(\pi_1, \pi_2, \pi_3) \quad [\text{Eq 2}]$$

in which $\pi_1 = ph^2/F$

$$\pi_2 = E/kh$$

$$\pi_3 = p/E$$

where

σ = tensile stress in the pavement slab (psi)

F = applied load (lbs)

h = pavement thickness (in)

p = contact pressure (psi)

E = modulus of elasticity of pavement slab (psi)

k = subgrade modulus (psi/in)

¹²H.L. Langhaar, *Dimensional Analysis and Theory of Models* (John Wiley & Sons, 1951).

The relationship between these dimensionless factors can be determined from Westergaard analysis of a plate supported on an elastic foundation. The Westergaard solution is expressed in Equation 1 from which Langhaar developed the relationships between π_1 , π_2 , and π_3 as:

$$\sigma = \frac{F}{h^2} f(\pi_1, \pi_2) \quad [\text{Eq 3}]$$

Thus Equation 2 becomes

$$\sigma \frac{F}{h^2} f \left(\frac{E_p^2 h^3}{kF^2} \right) \quad [\text{Eq 4}]$$

Thus Langhaar demonstrated that "Westergaard's theory can be represented by a single curve with $E_p^2 h^3 / kF^2$ as the abscissa and oh^2/F as the ordinate."

A single curve of this type was developed for typical prototype pavements using Corps of Engineers design criteria. Figure 20 shows a rigid pavement design curve for a single wheel gear fighter aircraft having a 100 sq in tire contact area and a wheel load of 25,000 lbs. The thickness requirements shown for B and C Traffic Areas represent varying repetitions and magnitudes of load. As suggested by Langhaar, a curve was prepared which would indicate the relationship between $E_p^2 h^3 / kF^2$ and oh^2/F for a series of prototype pavements. Variations in magnitude and repetitions of load are satisfied automatically as these changes are reflected by modifying the allowable stress as some percentage of the modulus of rupture. This unique solution is for jointed edge pavements. Such pavements will be in the initial failure condition at the end of their design life. A comparison of this predicted performance and the performance of the model pavements was then made by calculating the same dimensionless factors for all jointed edge model pavements. The dimensionless plot of the prototype pavements and the model pavements is shown on Figure 21. The line showing the prototype pavements shows the normal range of pavement thicknesses, stresses and subgrade reaction values which would be encountered with a 25,000 lbs single wheel gear load. Extrapolation of the prototype pavement line to the vicinity of the model pavement points would indicate that the Westergaard analysis would be a rather poor predictor for the model pavements.

An earlier study of prestressed model pavements¹³

conducted with the same test apparatus and with approximately the same slab thicknesses and subgrade moduli, correlated well with prototype prestressed pavements. A comparison of the failures experienced with the model pavements in this study and the prestressed model pavements shows some rather striking similarities. Figure 22 shows a close up view of a failed area on model test pavement number 6. Figure 23 shows a failed area from a prestressed pavement from the earlier test series referenced above. In both of the two photographs the failed areas were filled with crushed concrete. The crushed material was carefully removed prior to photographing the failed areas. The two photographs are quite similar except for the absence of the prestressing tendons in Figure 22. The similarity of failures and the superior performance of the model pavements led to an examination of possible mechanisms by which the model pavements may be experiencing spurious prestressing forces which are not considered in the Westergaard analysis.

The Westergaard analysis does not account for stresses generated by the elongation of the neutral axis (membrane action) or by the frictional restraint acting at the slab/subgrade interface. Using some simplifying assumptions, an analysis of the effects of membrane action and frictional restraint was performed to obtain an approximation of the magnitude of the stresses involved. The general equation for extreme fiber stress was assumed as follows:

$$\sigma = \frac{F}{h^2} f \left(\frac{E_p^2 h^3}{kF} \right) \pm M \mp R_f \quad [\text{Eq 5}]$$

where F, h, p etc. are as before and represent the Westergaard analysis

M = membrane stresses due to elongation of the neutral axis

R_f = stress due to subgrade frictional restraint.

The sign convention adopted for Equation 5 assumes tension on the bottom of the slab to be positive.

An approximation of the membrane stresses, M, was developed as follows. A first approximation of the deflected shape of a pavement on an elastic foundation was assumed to be a sine curve. The generated length of a sine curve over one half the period would be indicative of the total strain experienced along the neutral axis of the pavement. It can be shown that the

¹³ Small Scale Model Studies of Prestressed Rigid Pavements - Part I.

increased length of the sine curve, S , subtracted from the horizontal projection is equal to:

$$S - L = \frac{1}{4} \frac{W^2 \pi^2}{L} = \Delta L \quad [\text{Eq 6}]$$

where S = the length of the sine curve
 W = the amplitude of the sine curve
 L = the period of the sine curve
 $\pi = 3.14159$, transcendental number

The same relationship will hold true for any portion of a sine curve provided L is adjusted to reflect the proper interval of consideration. The average strain experienced along the neutral axis can then be approximated by:

$$\epsilon_{\text{ave}} = \frac{\Delta L}{L} = \frac{1}{4} \frac{W^2 \pi^2}{L^2} \quad [\text{Eq 7}]$$

The average stress, M , can be obtained from:

$$M = \frac{W^2 \pi^2}{4 L^2} E \quad [\text{Eq 8}]$$

where E = modulus of elasticity.

The elastic deflections of the model pavements agreed reasonably well with Westergaard's predictions. Thus, the amplitude term W in Equation 8 can be replaced with Westergaard's expression for deflection. Westergaard's equation for the maximum deflection of an edged loaded pavement is:

$$W = 0.433 \frac{F}{k l^2} \quad [\text{Eq 9}]$$

where W = maximum edge deflection due to a concentrated load

F = applied load

k = subgrade modulus

l = radius of relative stiffness

0.433 = constant involving unit width, moment of inertia and Poisson's ratio of 0.15

In the final form the applied load was multiplied by 0.75 to account for load transfer and the L term of Equation 8 was set at six times the radius of relative stiffness. The L term is an expression of the diameter

of the deflection basin which is about six times the radius of relative stiffness.

Equation 8 can thus be rewritten as follows:

$$M = \frac{0.00073 F^2 \pi^2 E}{k} \quad [\text{Eq 10}]$$

Equation 10 can be further simplified by substituting the equation for the radius of relative stiffness into Equation 10. The equation for the radius of relative stiffness is:

$$l^4 = \frac{E h^3}{12(1 - \mu^2) k} \quad [\text{Eq 11}]$$

Using 0.15 for Poisson's ratio and simplifying the final form for the approximate membrane stress is as follows:

$$.0086 \frac{F^2 \pi^2}{k l^2 h^3} \quad [\text{Eq 12}]$$

Where F , H , l etc have been previously defined.

An approximation of the stress due to subgrade frictional restraint, R_f , was also developed. The pressure exerted by the subgrade on the bottom of the slab is, by definition:

$$\sigma_N = Wk \quad [\text{Eq 13}]$$

where σ_N = normal stress exerted by subgrade on the slab

W = slab deflection

k = subgrade modulus

The available frictional restraining force should be equal to the normal force acting at the slab/subgrade interface multiplied by the coefficient of friction. Again using the first approximation of a sine curve for deflection and using an average value of amplitude for a sine curve of 0.636 and unit pavement width, the expression for frictional force becomes:

$$P_f = .2065 \frac{F L C_f}{l^2} \quad [\text{Eq 14}]$$

where P_f = frictional force

C_f = coefficient of friction

L , F are as previously defined.

Table 4

h in	Prototype k in/psi	F lbs	Bending Stress psi	Membrane Stress psi	Available Frictional Stress psi
9.8	200	25,000	526	.22	55
10.3	100	25,000	526	.25	42
10.6	50	25,000	526	.31	33
11.0	25	25,000	526	.37	25
Model					
1.53	200	2,368	1,834	8.5	298
1.00	120	1,805	3,030	43.2	520
1.23	114	1,503	1,878	12.1	268
1.50	96	2,520	2,212	15.2	226

Assuming this force to act across the depth of the pavement and thereby converting to a frictional stress requires division by the slab thickness, h . Tests conducted by the Public Roads Administration (presently the Federal Highway Administration) show the coefficient of friction is inversely proportional to the square root of slab thickness.¹³ An empirical equation was developed from force displacement tests in which the slabs were moved horizontally across the subgrade. The coefficient of friction thus obtained represents a maximum available at the point of impending motion. The expression developed from these tests is as follows:

$$C_f = .585 \sqrt{\frac{A}{h}} \quad [\text{Eq 15}]$$

where C_f = coefficient of friction

A = slab length in feet

h = slab thickness in inches

0.585 = empirical factor and units factor
to account for A being in feet
and h being in inches

Incorporating Equation 15 into Equation 14, describing L in terms of l , and allowing for load transfer across slabs yields the final frictional restraint equation:

$$R_f = \frac{.5436}{hl} \sqrt{\frac{A}{h}} \quad [\text{Eq 16}]$$

The complete state of stress in a pavement under a single wheel load can thus be approximated by combining Equations 4, 12, and 16. It should be noted that Equations 12 and 16 will yield average values since the average value for the sine curve approximation was used in their development. Equation 16 is also dependent upon incipient motion occurring at the slab subgrade interface.

Table 4 compares the stresses in prototype pavements with selected model pavements. The prototype pavements were selected from the design curve for single wheel aircraft, Figure 20. The model pavements were four arbitrarily selected jointed edge pavements without stabilized elements. Tests 15, 16, 17 and 18 (see Table 1) were the tests selected.

The table illustrates the approximate range of stresses encountered with the model pavements as compared with those of prototype pavements. It should be noted that the bending stresses shown are maximum values and the membrane and frictional stresses are average values.

The normal range of prestress used for pavements is on the order of 200 to 400 psi, therefore, the values shown in Table 4 are significant for the model pavements. The material presented above was considered sufficient basis for using an analysis which assumes full friction is developed at each interface to analyze the model pavements. The method of analyzing prestressed pavements was not considered applicable as there is no way to predict how much of the available frictional restraint stress is mobilized as prestress. Back calculation indicates between 25 and 50 percent of the available frictional stress was mobilized

¹³Small Scale Model Studies of Prestressed Rigid Pavements—Part I.

in the model pavements. The method of analyzing prestressed pavements does not have provision for a layered foundation which was also considered to be a serious drawback in analyzing the pavements which contained a stabilized element.

All rigid pavement test pavements were analyzed using an elastic layered computer code developed by the Chevron Company and modified by the University of Illinois to allow free form data input. This elastic layered program allows for the inclusion of the concrete floor supporting the entire model, the subgrade soil, the stabilized element and the pavement slab. The analysis assumes that no slippage occurs between the layers, i.e., the strain in the bottom fibers of the upper layer and strain in the top fibers of the layers immediately below are equal. The program was developed to analyze layered pavement structures under static loading. The solution also assumes the layers are all infinite in horizontal extent with no discontinuities such as cracks or joints. To analyze pavements constructed with a free edge or a jointed edge, it was necessary to use the results of the instrumentation readings, strain data in particular. Strains were measured and compared at the free edge and the slab interior. Ratios of these strains indicated the strain and presumably the stress at a free edge was 115 percent of the interior stress. Therefore, stresses computed by the layered pavement program were adjusted to reflect the increase in stress due to a free or jointed edge.

The results of these analyses are compared with the full scale prototype design line. The design factor as the ordinate of Figure 24 is computed by dividing the flexural strength of the paving material by the maximum load induced stress. The layered analysis, as would be expected, showed an increase in flexural stress in the stabilized material as the modulus of elasticity of the stabilized material increased. For the cement stabilized material, the flexural stress in the stabilized element was the controlling stress rather than the portland cement concrete stress. This indicates the pavements containing cement stabilized elements act as overlay pavements with the slab and stabilized element both contributing flexural capacity to the pavement structure. The layered analyses of pavements containing lime and bituminous stabilized elements show practically no capacity for flexural stresses but merely serve to increase the capacity of the foundation to accept normal forces. This behavior is characterized by an increase in subgrade modulus rather than an overlay system.

In the plot of design factor versus coverages, the portland cement concrete stress levels are plotted in all cases except for the cement stabilized materials which show the stress level for the stabilized element. The number of coverages on the abscissa is the number of coverages necessary to produce the initial failure or first top surface crack. These data are presented on Figure 24. The data, in general, tend to fall below the prototype design line, as expected. The design line has been established from full scale tests of prototype pavements and is actually an upper bound for the observed failures. Being an upper bound, rather than an average or central tendency indication, some degree of conservatism is provided automatically. Also, the prototype pavements were full scale test tracks and were thus subjected to climatic conditions which are not present in the model. The lack of environmentally induced stresses and strains in the model would tend to promote better than anticipated performance from the model as the pavements were constructed and tested under ideal laboratory conditions.

Flexible Pavement Tests. No dimensional analyses were performed for the flexible pavement tests as nondimensional plots have been prepared from prototype tests of flexible pavements previously. The models tested were consistently within the range of values of these nondimensional plots and were considered representative of prototype behavior, not requiring an adjustment for size effects.

The flexible pavement model tests were analyzed using the standard CBR method of analysis which is applicable to flexible pavements. The CBR method of design and analysis has evolved over the past 20 or so years and has been substantiated by the testing of many prototype test pavements under simulated aircraft loadings. Sufficient data have been collected to establish a nondimensional plot of the ratios of CBR over applied tire pressure versus the thickness required for 5,000 coverages over the square root of the tire contact area. This plot is included in Figure 25. Using the plot, it is possible to establish the total thickness of flexible pavement required over a given subgrade CBR necessary to withstand 5,000 coverages of a given wheel load (identified by pressure and contact area). Other traffic volumes can be analyzed by using an empirically developed relationship which relates traffic volume to the percentage of the 5,000 coverage thickness. This relationship is shown as Figure 26. The relationship between percent design thickness and coverages is shown as a dashed line for 25,000

coverages or more because empirical validation of the line beyond 25,000 coverages has not been established, and this portion is an extrapolation of lower traffic volume data.

The model test pavements were analyzed using the following procedure as an example:

Flexible Test Pavement 6

Subgrade CBR	=	5
Wheel Load	=	1559 lbs
Tire Pressure	=	70 psi
Contact Area	=	$1559/70 = 22.3 \text{ in}^2$
CBR/p	=	$5/70 = 0.0714$
from Figure 1/ \sqrt{A}	=	1.20 for 5,000 coverages
\sqrt{A}	=	4.72
1	=	5.66 inches for 5,000 coverages
Actual 1	=	2.25
Percent of 5,000 coverage thickness	=	$\frac{2.25}{5.66} = 40\%$

40% thickness would correspond to 12 coverages from Figure 26. All test pavements were analyzed in this manner using the subgrade CBR measurement. The results of this analysis are shown graphically on Figure 27. The pavements without a stabilized element are shown as circles and the pavement with stabilized elements are shown as triangles. The test results generally agree with the results predicted by CBR analysis. The pavements which fall below and to the right of the design line were trafficked to a more severe state of distress than would be tolerated on an operational pavement. Only those pavements which experienced failure in the subgrade material and the stabilized layer are plotted. The first three flexible pavement tests failed entirely within the base course due to the high contact pressures under the cushion tire which exceeded the stability of the base course.

Visual observations of pavement performance and results of CBR tests indicate some benefit is derived from the use of lime stabilized and bituminous stabilized layers in flexible pavements over an equal thickness of crushed stone base course. Some increase in the CBR value will be noted and the change in performance will be commensurate with the increased CBR value. Elastic layered analyses of flexible pavements containing cement stabilized elements show that the location of the stabilized element within the pavement structure determines the extent of flexural behavior the element will exhibit. Stabilized elements

below a layer of crushed stone base course tend to exhibit less flexural action since the load is already spread to some extent before it reaches the stabilized element.

Due to the limited capacity of the loading rig, the stabilized elements tested in the program were rather thin. Thicker sections probably would have exceeded the load capacity of the device and could not have been failed. The standard field CBR test¹⁴ was used to evaluate the strength of the subgrade and the stabilized layers. The ratio of loaded area radius to stabilized layer thickness was much greater than would be encountered in the prototype. The use of a scaled piston was considered; however, because of the lack of performance data using a smaller piston the idea was dropped. The effects of evaluating a prototype stabilized layer, where the thickness of the layer is large relative to the radius of the CBR piston, cannot be evaluated from these tests. CBR tests on cement stabilized materials, in particular, may not yield reasonable results where the stabilized elements are three inches or greater in thickness.

Discussion. The poor correlation between the model and prototype rigid pavements using the Westergaard analyses is primarily due to the subgrade frictional restraint stresses. Analysis of the model tests using a layered mathematical model which assumes full friction at all interfaces and comparing with a frictionless analysis for the prototype improves the correlation considerably. Some disparity between the model and prototype can be expected due to the lack of environmental effects acting on the model slabs. The analysis was performed using E values for the soil as determined from CBR tests, unconfined compression tests, plate bearing tests and engineering judgement. Some correlations have been established between E value and the tests above by Thompson. Wide ranges of E values can be obtained from the various correlations available and the selection of the proper E becomes a matter of judgement. The test data points can be shifted significantly by altering the E value of the soil layers. The elastic layered approach seems most reasonable for pavements containing stabilized layers if realistic values for the modulus of elasticity of the various layers can be determined.

¹⁴ Application of the Results of Research to the Structural Design of Concrete Pavements, Proceedings of the American Concrete Institute, Vol 35 (September 1939).

6 CONCLUSIONS, RECOMMENDATIONS AND CLOSURE

Conclusion. Based on the test results reported herein the following conclusions are drawn regarding the structural benefits imparted to a pavement structure by various stabilized elements.

Rigid Pavement Test Series.

(1) **Applicability of Theory.** The Westergaard analysis did not yield reasonable results for the model pavements tested in this study. The major drawback in applying the Westergaard analysis to a pavement structure containing a stabilized element lies in the assumption of a Winkler foundation and the ability to analyze only a single plate on the foundation. Inclusion of a stabilized layer can only be accomplished by modifying the spring constant of the subgrade, modifying the thickness of the concrete slab or by some combination of modifications to the subgrade and slab.

(2) **Lime Stabilization.** Lime stabilization used in conjunction with a rigid pavement appears to increase the bearing capacity of the subgrade. An analysis of a rigid pavement containing a lime stabilized layer by the Westergaard method should reflect the effect of the lime stabilized element by an increase in the subgrade modulus. Lime stabilized layers do not contribute appreciably to the flexural capacity of the structure due to the low modulus of elasticity relative to that of the pavement slab.

(3) **Cement Stabilization.** Cement stabilized layers possess sufficient rigidity to contribute to the flexural capacity of the structure. Rigid pavement structures containing cement stabilized element should be treated as overlay pavements. Cement modified soil layers appear to merely improve soil workability but do not increase the structural capacity of rigid pavement structures.

(4) **Bituminous Stabilization.** The bituminous stabilized layers tested in this study offered no advantage over high quality crushed limestone base courses.

Flexible Pavement Test Series.

(1) **Applicability of Theory.** For the tests conducted in this study, the CBR analysis yielded reasonable results. Apparently the stabilized materials had no greater capacity for supporting traffic than a conventional base course of the same CBR.

(2) **Lime Stabilization.** The lime stabilized layers seemed to offer little or no performance benefits over an equal thickness of high quality crushed limestone. The performance of the layer should be reflected by the CBR value of the layer.

(3) **Cement Stabilization.** The ability of the cement stabilized layer to contribute flexural capacity to the pavement structure depends on its location in the structure. Cement stabilized layers located at or near the top surface will behave as slabs, however, these same layers located beneath a base course cover will be too far removed from the load to exhibit flexural action. Cement modification of soils appears to merely improve soil workability but does not contribute to the structural capacity of the pavement.

(4) **Bituminous Stabilization.** The bituminous stabilized layers offered no advantage over high quality crushed limestone base courses.

Recommendations. The following recommendations are offered relative to the design and evaluation of pavement structures incorporating stabilized elements based on the results of this study.

(1) The elastic layered method of analysis is recommended for prototype pavements containing stabilized elements. Field applications should be based on a friction free interface assumption.

(2) The use of equivalency factors between base course materials and cement stabilized layers is discouraged. The behavior of the two materials under load is completely different and a true equivalency is not possible.

(3) Should an actual application require the use of a very thin slab supported on a subgrade, exploitation of the frictional restraint stress is not recommended. Environmental factors acting on a slab, such as ingress of moisture at the subgrade interface and warping due to temperature gradients, will probably reduce the frictional restraint to a very low level.

Closure. The following observations were made during the course of this study. While these comments are not directly supported by definitive data, they are considered to be of value and are offered for consideration.

(1) An exhaustive dimensional analysis and similitude study should precede any model test of pavement structures. Rigid pavement models in which the slab thickness is less than about 4 inches will result in a magnification of subgrade frictional restraint stresses.

(2) Care should be exercised in locating a stabilized element in a pavement structure so as not to impede drainage of the structure. In general, stabilization tends to reduce the permeability of materials. Analytically and under idealized conditions, some layer arrangements will appear superior in regard to structural support but will offer formidable drainage problems.

(3) The use of bituminous stabilization of marginal materials should be investigated. For example, an

aggregate base course material which deviates from the recommended gradation specifications may be improved sufficiently by bituminous stabilization to offer satisfactory performance.

(4) If the elastic layered method of analysis is adopted for pavement structures, further research is recommended for the determination of elastic constants of paving materials with reasonable ease, accuracy and reliability.

REFERENCES

- Ahlberg and Barenberg, *Pozzolanic Pavements*, Engineering Experiment Station Bulletin 473, (University of Illinois, February 1965).
- Ahlberg and Barenberg, *The U of I Pavement Test Track - A Tool for Evaluating Highway Pavements* (University of Illinois Engineering Experiment Station, January 1963).
- Application of the Results of Research to the Structural Design of Concrete Pavements, *Proceedings of the American Concrete Institute*, Vol 35 (September 1939).
- Kawala, E.L., *Cement Treated Subbases for Concrete Pavements*, Technical Bulletin 235, (American Road Builders Association, 1958).
- Kawala, E.L., "Cement Treated Subbase Practice in U.S. and Canada," *ASCE Proceedings, Highway Division Journal HW-2*, (October 1966).
- Langhaar, H.L., *Dimensional Analysis and Theory of Models*, (John Wiley and Sons, 1951).
- Load Tests on Rigid Airfield Pavements Constructed on Stabilized Foundations*, Unpublished Memorandum Report (Corps of Engineers, Ohio River Division Laboratories).
- Losberg, Anders, *Structurally Reinforced Concrete Pavements*, (Chalmers University of Technology, Goteborg, 1960).
- Military Standard 621-A*, Test Methods for Pavement Subgrade, Subbase and Base-Course Materials.
- Myerhof, J.J., "Load Carrying Capacity of Concrete Pavements," *ASCE Proceedings*, Vol 88, No. SM-3 Part I, (June 1962).
- Small Scale Model Studies of Prestressed Rigid Pavements - Part I, Development of the Model and Results of Exploratory Tests*, Technical Report No. 4-13/AD 281580 (Ohio River Division Laboratories, May 1962).
- Soil Testing Service, Inc., *Thickness Design Procedure for Airfields Containing Stabilized Pavement Components*, prepared for the Federal Aviation Agency, Contract No. ARDS-468, AD 607331.
- Thompson, M.R., "Lime-Treated Soils for Pavement Construction," *ASCE Proceedings, Highway Division Journal HW-2*, (November 1968).
- Westergaard, H.M., *Stresses in Concrete Pavements Computed by Theoretical Analysis*, Highway Research Board Paper (December 1925).

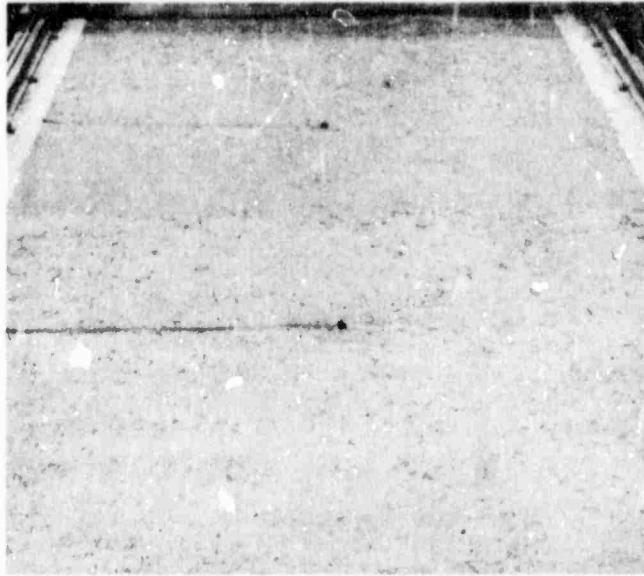


Figure 1. Completed subgrade prior to placement of polyethylene sheeting. (Material in the foreground is lime stabilized clay. The two small black tubes in the upper center of the photo are instrumentation housings with strings attached to pull wiring.)



Figure 2. Coating of crack alarm grid wires with epoxy resin prior to concrete placement.

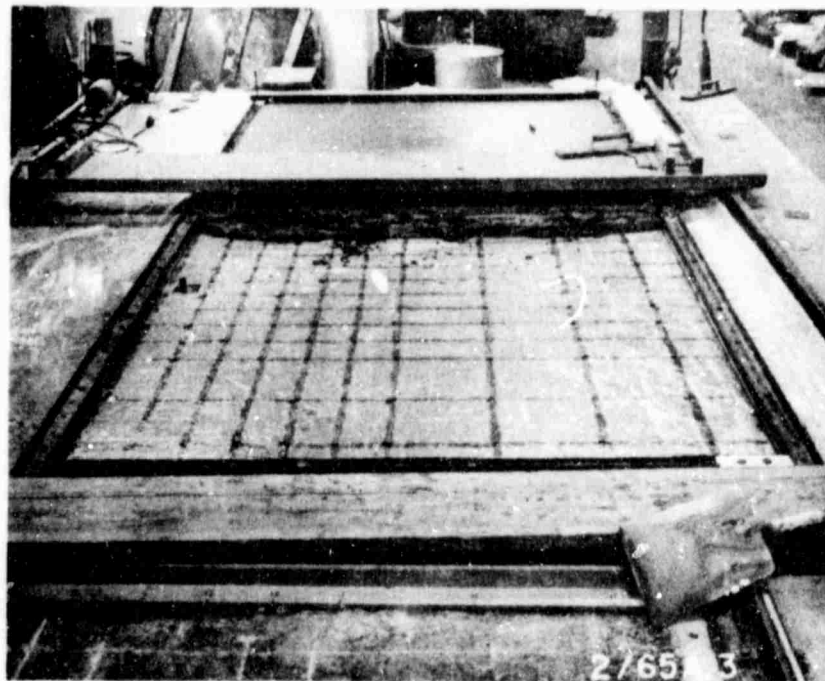


Figure 3. Concrete placement approximately one half complete (All crack alarm grid wires have been coated with epoxy resin.)



Figure 4. Vibrating pan type compactor used to compact crushed stone base course material for flexible pavement tests.



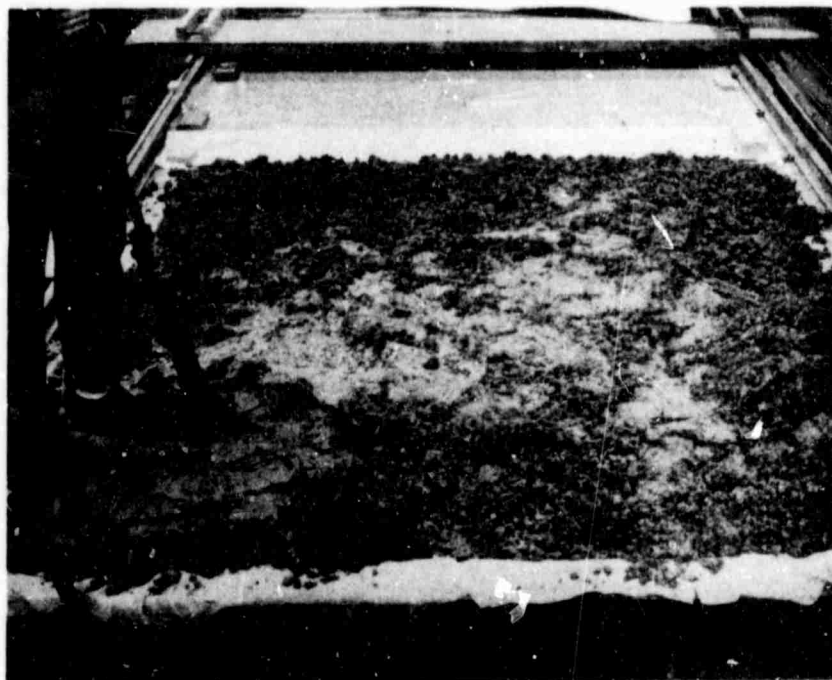


Figure 5. Compaction of the lime soil mixture with the pneumatic tamper.

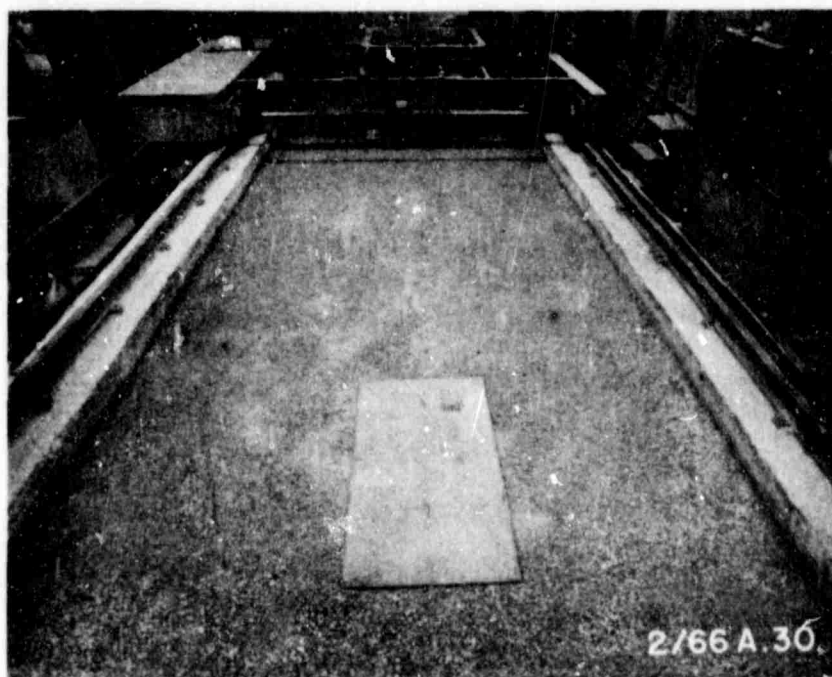


Figure 6. Overall view of a completed flexible pavement prior to test traffic.

LVDT MOUNTING

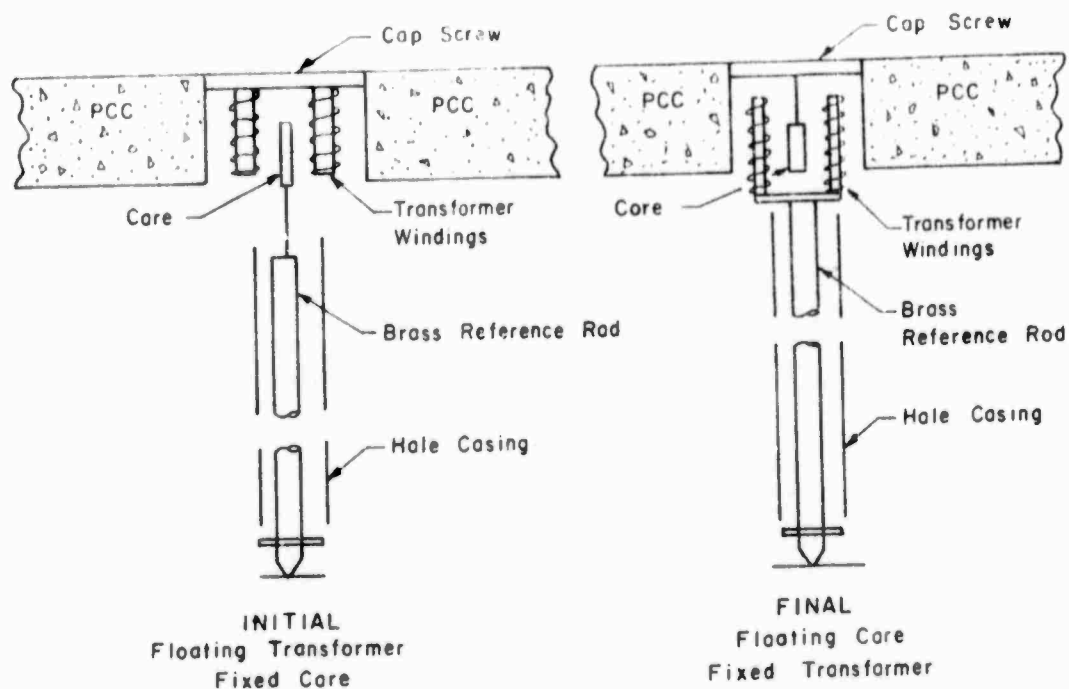


Figure 7. Linear variable differential transformer mounting techniques.

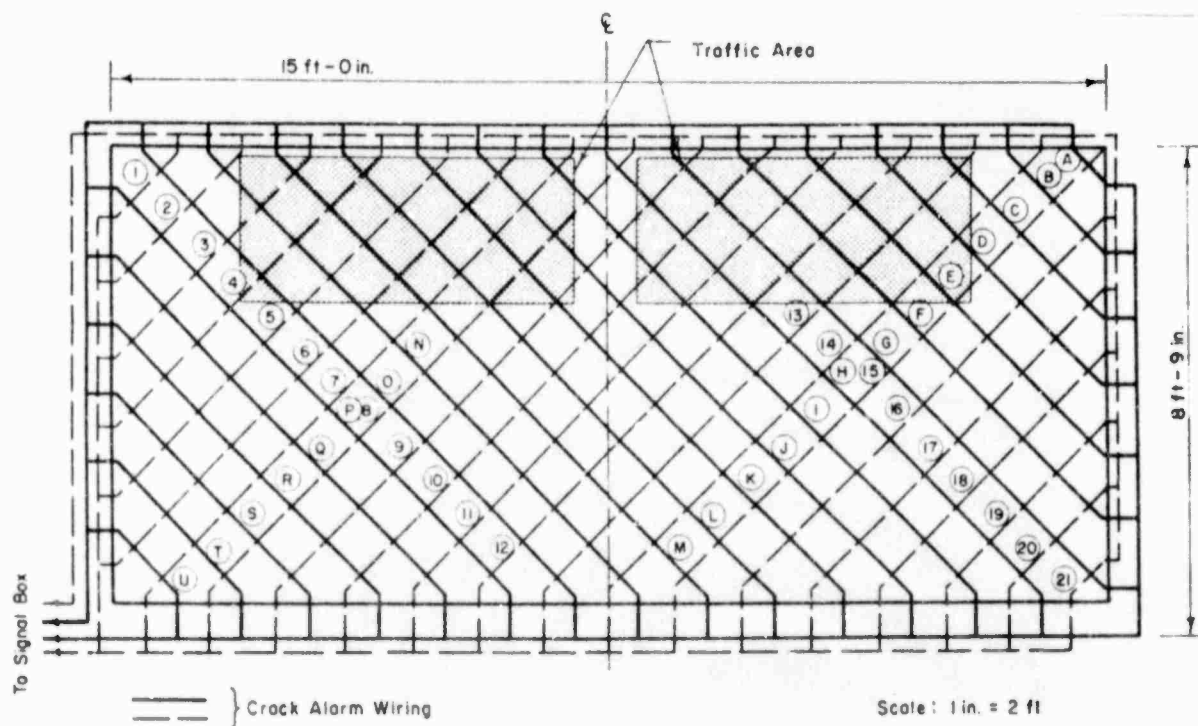


Figure 8. Typical layout of crack alarm wire grid.

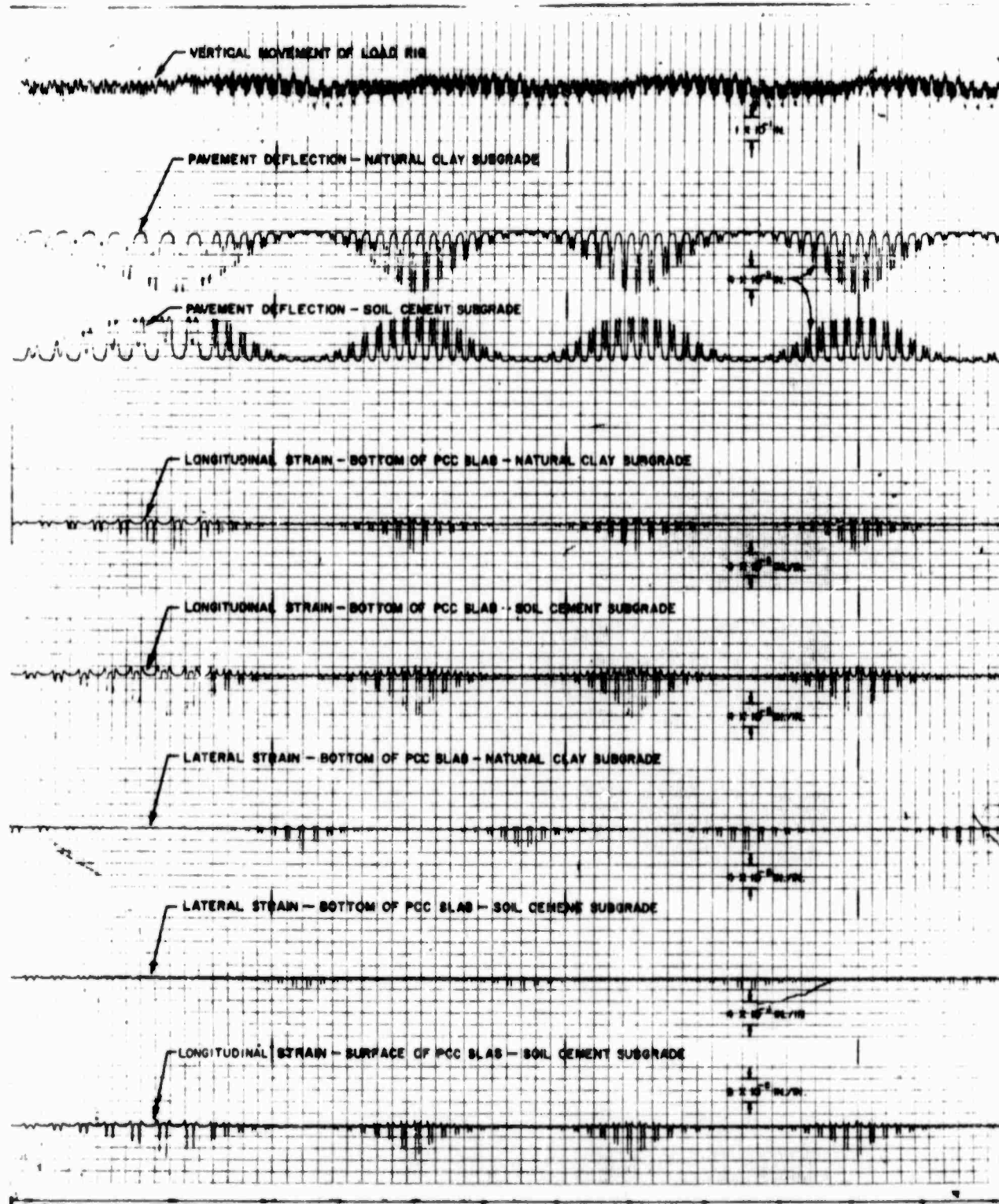


Figure 9. Typical oscillograph trace from traffic testing of model pavement 12.

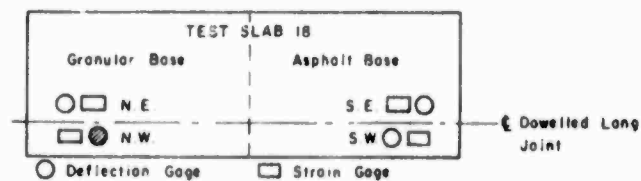
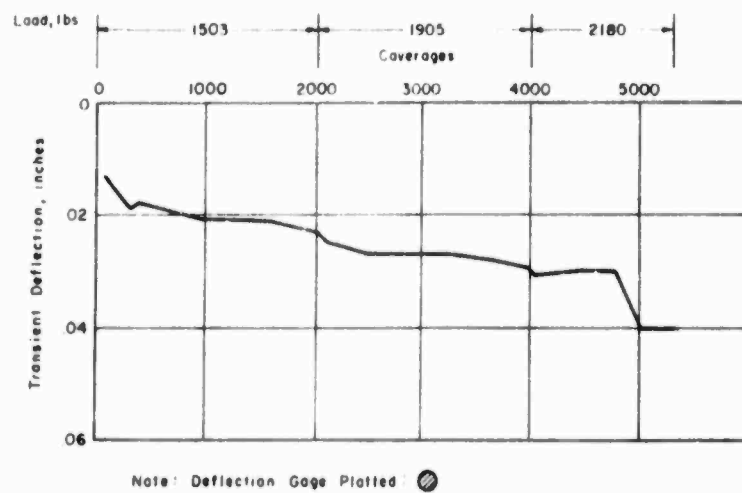


Figure 10. Typical deflection-coverage plot, west slab, nonstabilized.

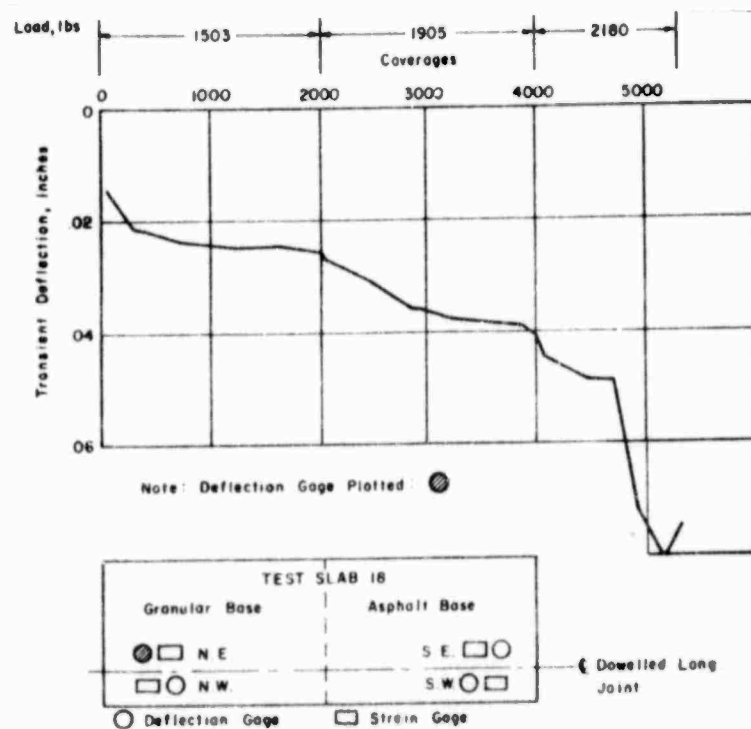


Figure 11. Typical deflection-coverage plot, east slab, nonstabilized.

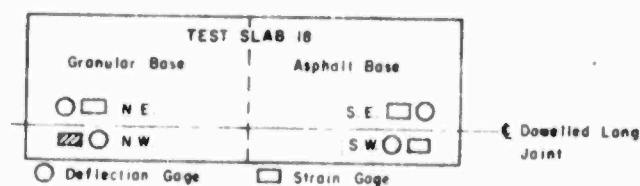
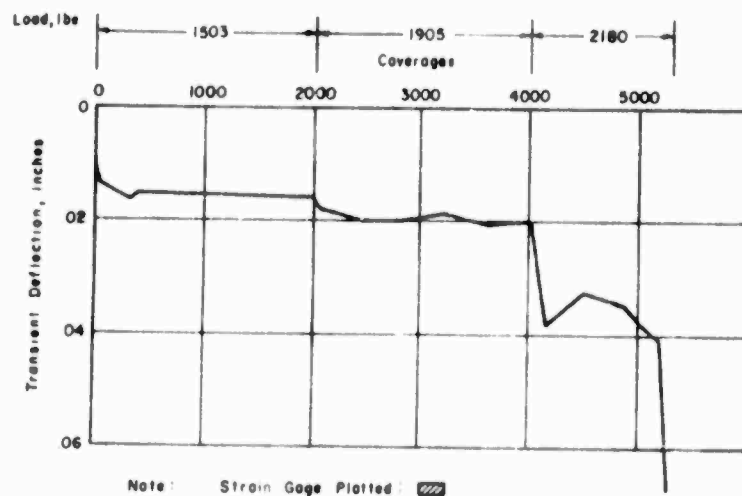


Figure 12. Typical strain-coverage plot, west slab, nonstabilized.

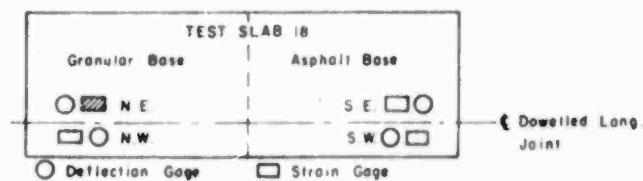
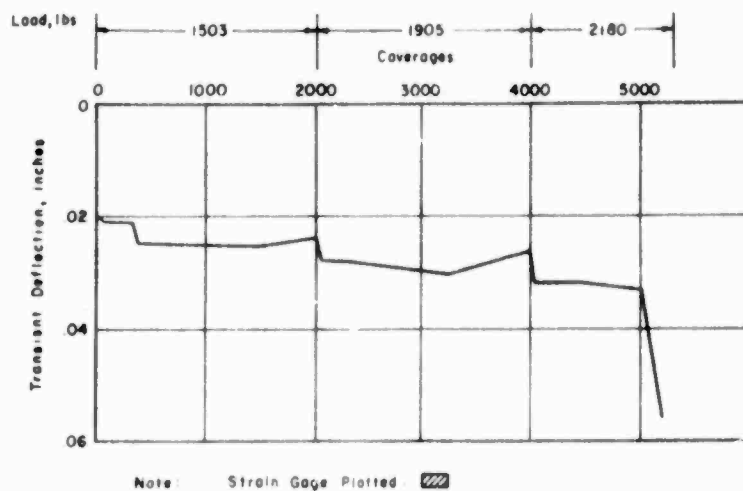


Figure 13. Typical strain-coverage plot, east slab, nonstabilized.

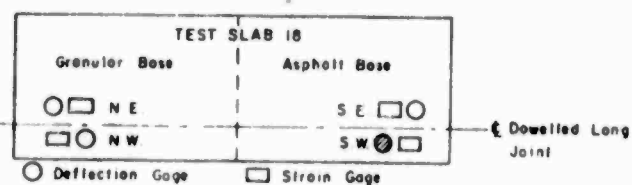
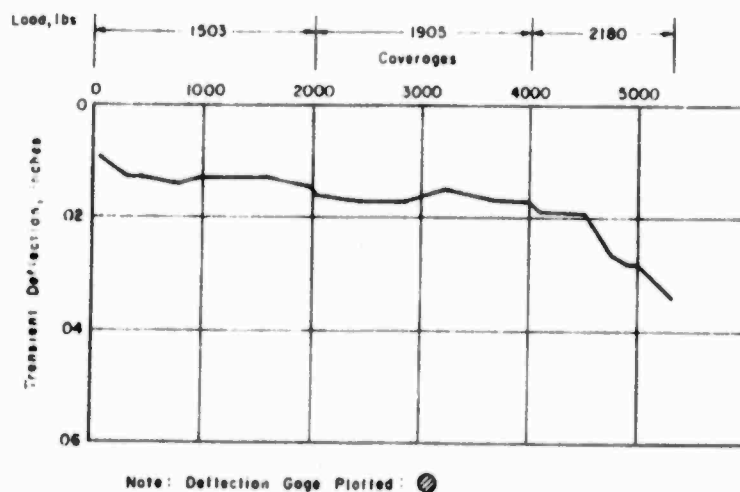


Figure 14. Typical deflection-coverage plot, west slab, stabilized.

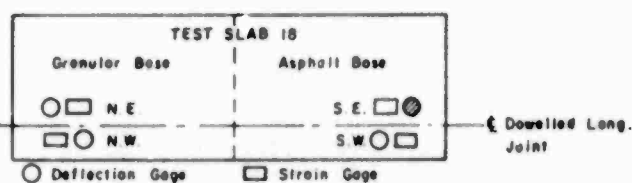
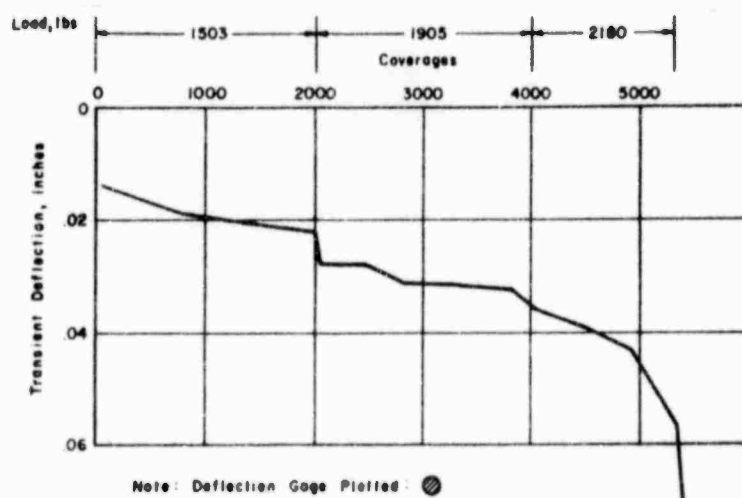


Figure 15. Typical deflection-coverage plot, east slab, stabilized.

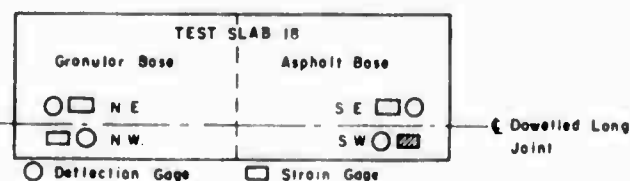
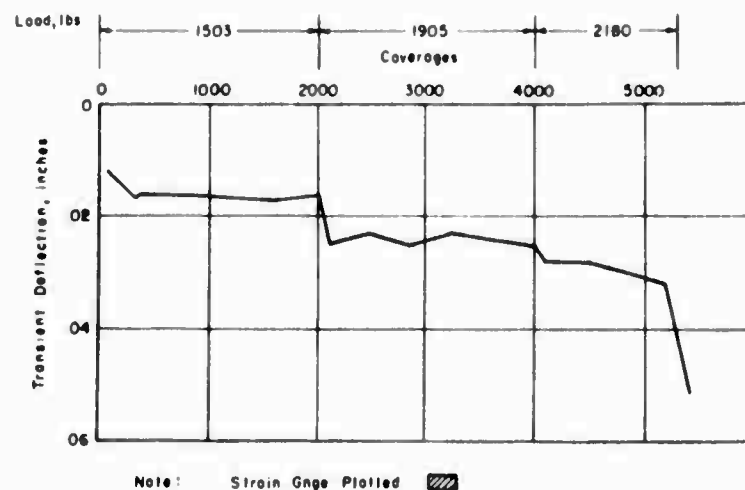


Figure 16. Typical strain-coverage plot, west slab, stabilized.

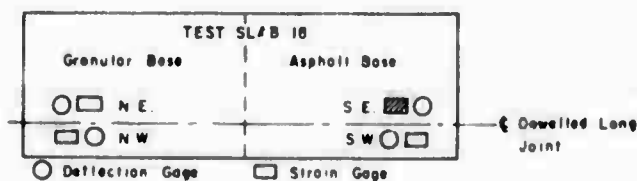
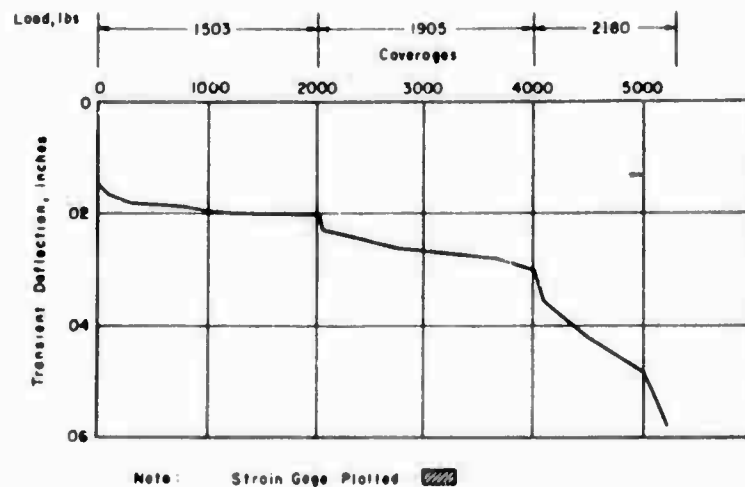


Figure 17. Typical strain-coverage plot, east slab, stabilized.

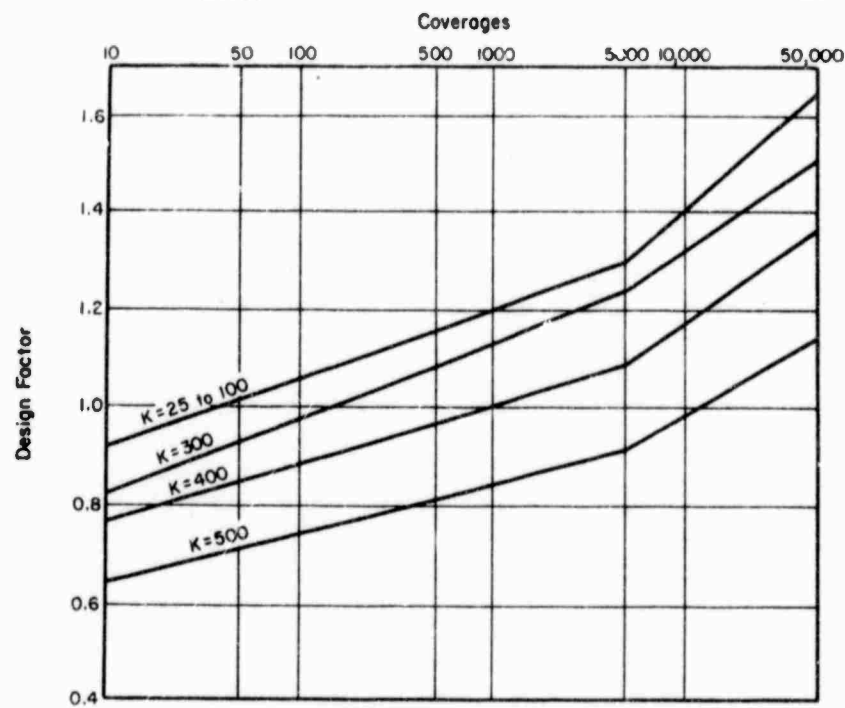


Figure 18. Design factor versus coverages for initial slab failure.

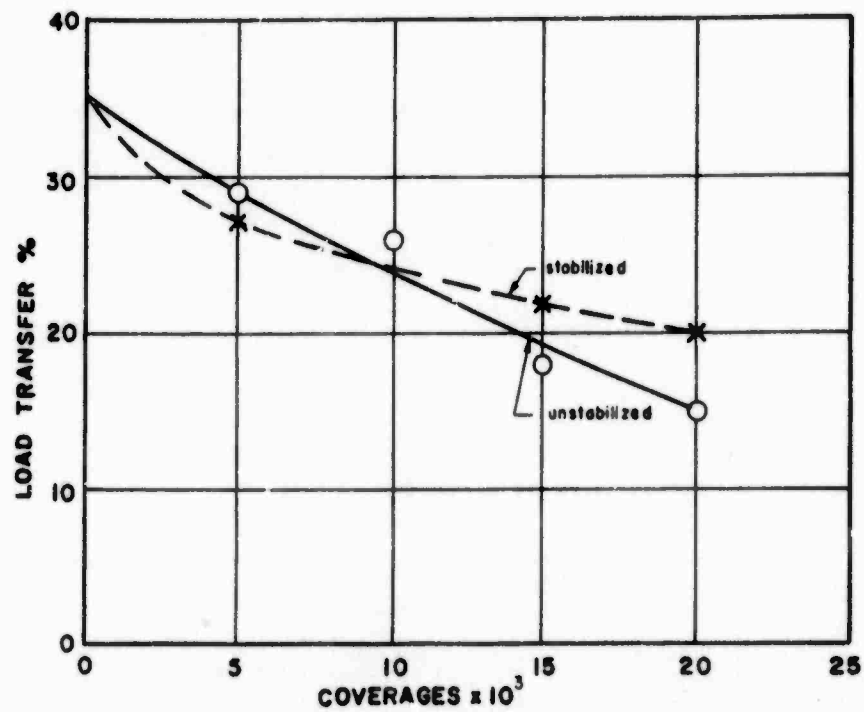


Figure 19. Typical summary of load transfer tests across joint.

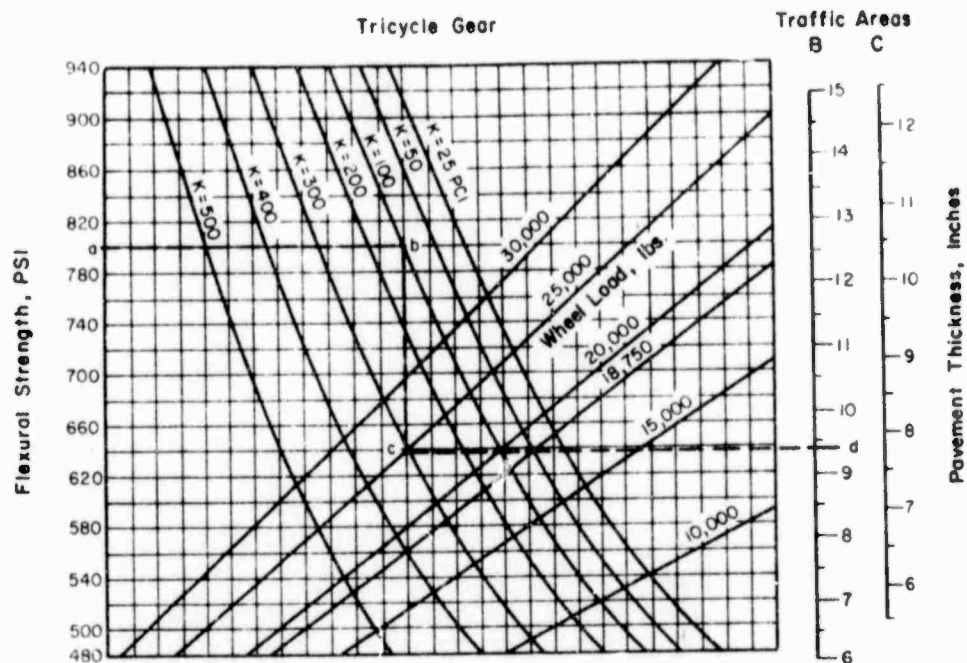


Figure 20. Design curves for concrete airfield pavements, single wheel, 100 sq. in. contact area.

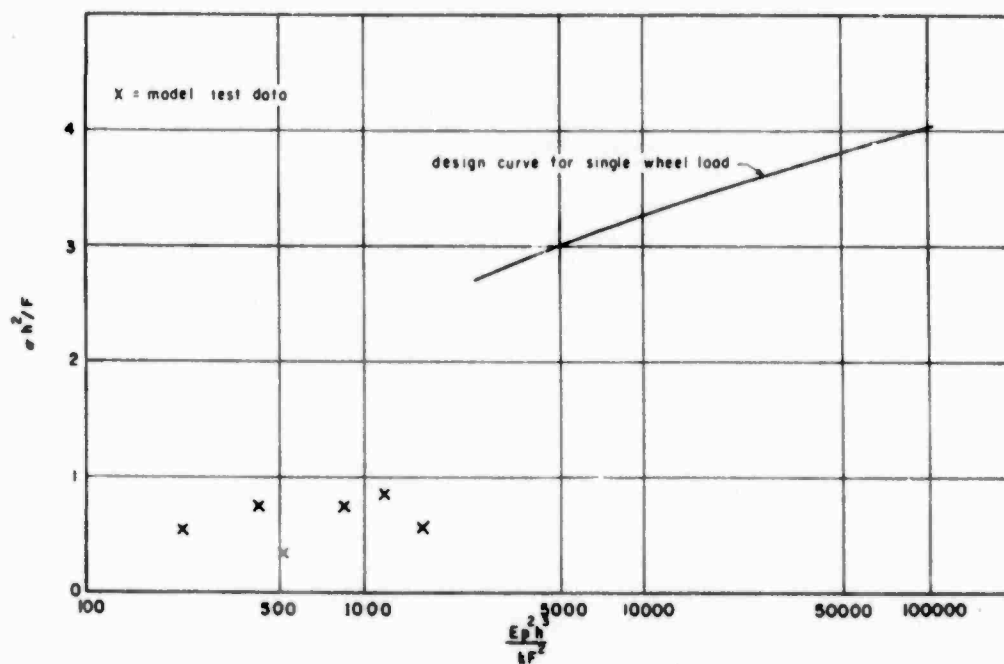


Figure 21. Nondimensional plot of single wheel design curve and model test data using Westergaard analysis.



Figure 22. Close-up view of a failed area on model test 6. (Crushed surface concrete was removed from the area prior to taking the photograph)

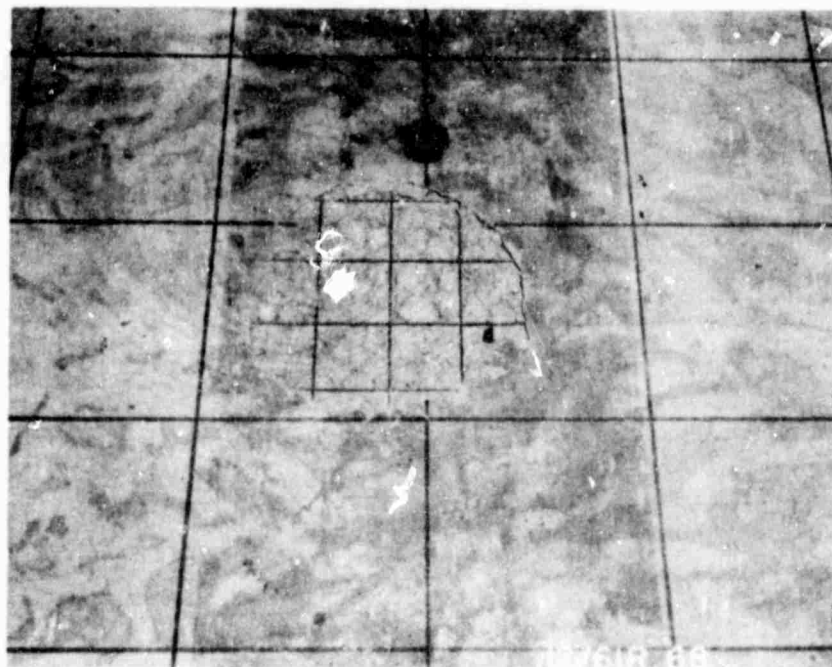


Figure 23. Close-up view of a failed area on a prestressed model pavement. (Crushed surface concrete was removed exposing the prestressing steel tendons.)



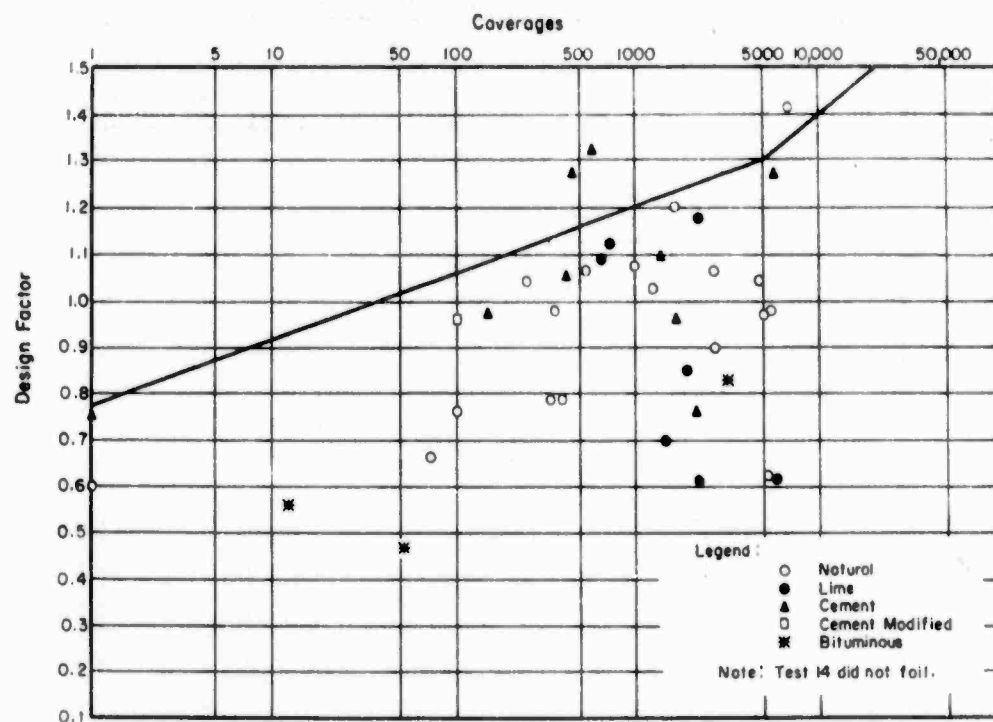


Figure 24. Summary of rigid pavement tests.

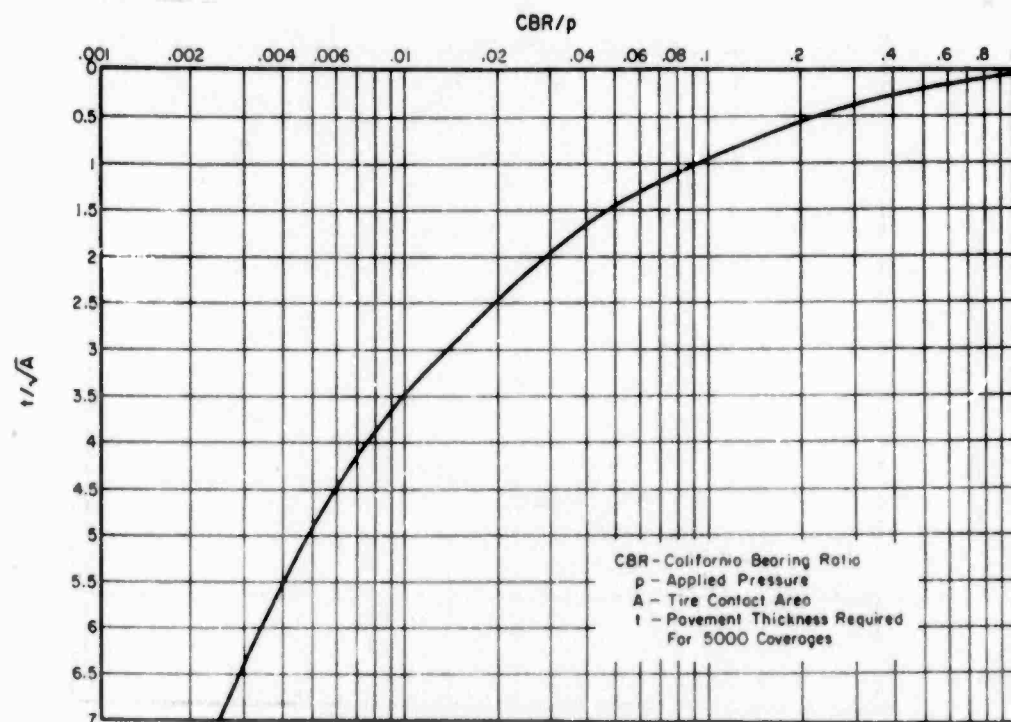


Figure 25. Consolidated CBR curve for 5,000 coverages.

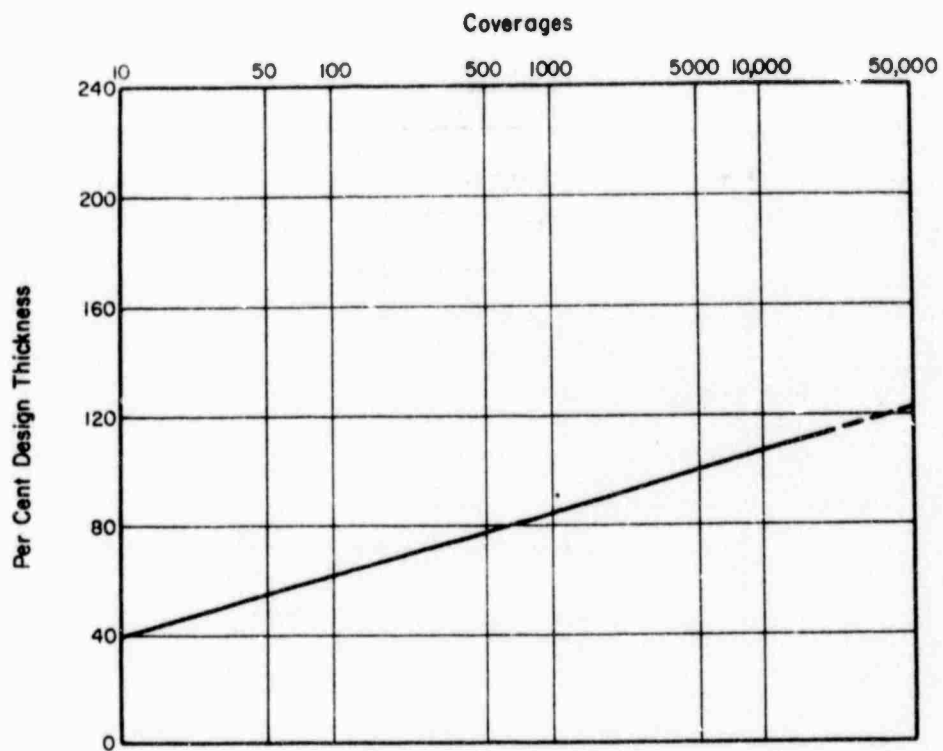


Figure 26. Percent design thickness versus coverages, flexible pavement failure.

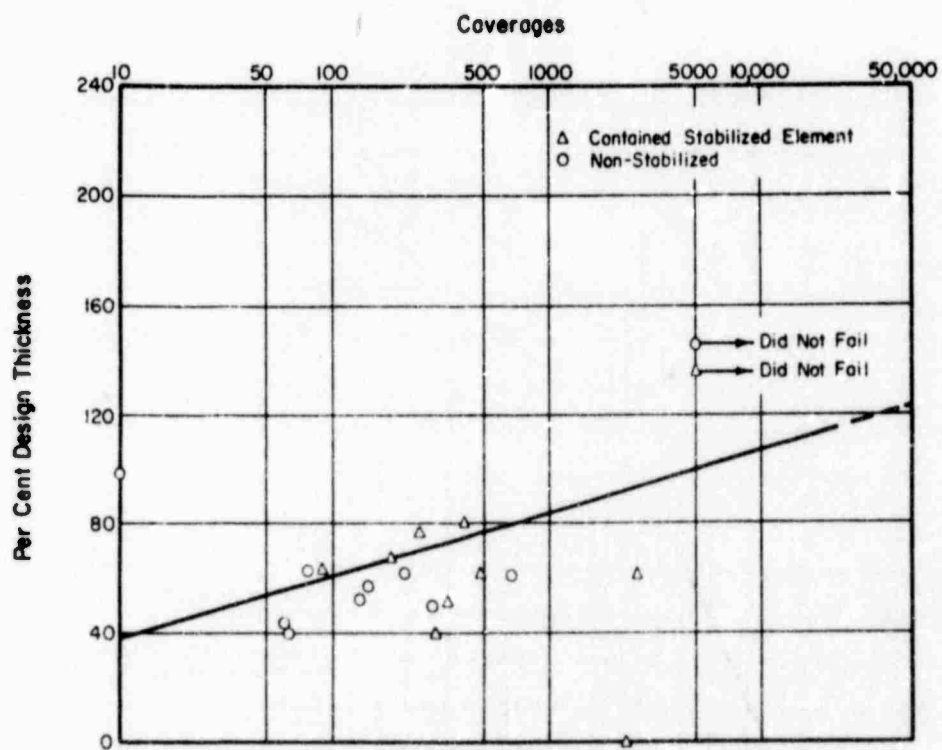


Figure 27. Summary of flexible pavement tests.